The effect of a partial resistive shell on the magnetohydrodynamical stability of tokamak plasmas

Richard Fitzpatrick

Citation: Physics of Plasmas (1994-present) **4**, 4043 (1997); doi: 10.1063/1.872525
View online: http://dx.doi.org/10.1063/1.872525
View Table of Contents: http://scitation.aip.org/content/aip/journal/pop/4/11?ver=pdfcov
Published by the AIP Publishing

The effect of a partial resistive shell on the magnetohydrodynamical stability of tokamak plasmas

Richard Fitzpatrick
Institute for Fusion Studies, Department of Physics, The University of Texas at Austin, Austin, Texas 78712

(Received 23 May 1997; accepted 7 July 1997)

A comprehensive theory is developed to determine the effect of a partial resistive shell on the growth rate of the external kink mode in a low-β, large aspect-ratio, circular flux-surface tokamak. In most cases, it is possible to replace a partial shell by a complete ''effective shell'' of somewhat larger radius. In fact, the radius of the effective shell can be used to parametrize the ability of a partial shell to moderate the growth of the external kink mode. It is necessary to draw a distinction between ''resonant shells,'' for which the eddy currents excited in the shell are able to flow in unidirectional continuous loops around the plasma, and ''nonresonant shells,'' for which this is not possible. As a general rule, resonant shells perform better than similar nonresonant shells. The theory is used to derive some general rules regarding the design of incomplete passive stabilizing shells. The theory is also employed to determine the effectiveness of two realistic feedback stabilization schemes for the resistive shell mode, both of which only require a relatively small number of independent feedback controlled conductors external to the plasma. © *1997 American Institute of Physics.* [S1070-664X(97)03211-4]

I. INTRODUCTION

The influence of a *complete* external resistive shell on the magnetohydrodynamical (MHD) stability of a toroidal pinch plasma has been extensively studied in the magnetic fusion literature.[1–27] It is well established that eddy currents induced in the shell can moderate the growth of an otherwise ideally unstable external kink mode, so that it evolves on the characteristic L/R time of the shell, instead of a much shorter time scale determined by plasma inertia. Such slowed down modes are usually referred to as ''resistive shell modes.'' Stabilization of the resistive shell mode is vital to the success of the ''advanced tokamak'' concept,[28] which aims to simultaneously maximize the plasma beta,[29] the energy confinement time, and the fraction of the current due to the noninductive bootstrap effect.[30] The eventual aim is, of course, to design an attractive fusion power plant which can operate in steady state, at high fusion power density, with low recirculating power.[31] The interaction of a rotating magnetic island (i.e., the nonlinear phase of a conventional tearing mode[32,33]) with eddy currents induced in the shell generates a nonlinear slowing down torque which effectively brakes the rotation once a critical island width is exceeded.[21,24] This effect is of importance because a nonrotating (or ''locked'') tearing mode is generally more unstable than an analogous rapidly rotating tearing mode (and, hence, the saturated island width is larger in the former case), since the latter mode is unable to penetrate through the shell.[11]

The aim of this paper is to develop a comprehensive theory of the interaction of MHD instabilities of a large aspect-ratio, low-β, tokamak plasma[34] (in particular, external kink modes) with a *partial* resistive shell. This investigation is relevant to magnetic fusion plasma physics because some existing tokamaks possess partial shells (for instance, the Princeton Beam Experiment, PBX-M,[35] and the Columbia High Beta Tokamak, HBT-EP[36]). Moreover, advanced tokamak designs invariably incorporate close fitting passive stabilizing shells with incomplete poloidal and toroidal coverage.[37] Finally, in most tokamak reactor designs the ''first wall'' is constructed out of some highly conducting material, and is both modular in nature and partial in coverage.[38] This investigation is also relevant to the feedback stabilization of MHD instabilities using a set of external windings with incomplete poloidal and toroidal coverage.

II. PRELIMINARY ANALYSIS

A. Introduction

Consider a large aspect-ratio, low-β, tokamak plasma whose magnetic flux surfaces map out (almost) concentric circles in the poloidal plane. Such a plasma is well approximated as a periodic cylinder. Suppose that the minor radius of the plasma is a. Standard cylindrical polar coordinates (r,θ,ϕ) are adopted. The system is assumed to be periodic in the z direction, with periodicity length $2\pi R_0$, where R_0 is the simulated major radius of the plasma. It is convenient to define a simulated toroidal angle $\phi = z/R_0$.

B. Basic definitions

The perturbed magnetic field is written as

$$\delta\mathbf{B} = \nabla\wedge(\psi\hat{\mathbf{z}}) \equiv \nabla\psi\wedge\hat{\mathbf{z}}, \tag{1}$$

where $\psi(r,\theta,\phi)$ is the perturbed poloidal magnetic flux. The magnetic field can only be written in this form provided that

$$\left|\frac{1}{r}\frac{\partial\psi}{\partial\theta}\right| \gg \left|\frac{1}{R_0}\frac{\partial\psi}{\partial\phi}\right|. \tag{2}$$

Suppose that the plasma is surrounded by a concentric cylindrical shell made of a rigid conducting material such as a metal. For the sake of simplicity, the analysis is performed in the ''thin shell'' limit, in which the skin depth of the perturbed magnetic field in the shell material is much greater than the thickness of the shell but much less than its radius.

In this limit, there is negligible radial variation of the perturbed flux ψ across the shell. It is, therefore, possible to unambiguously define a ''shell flux,''

$$\Psi_w(\theta,\phi)\equiv\psi(r_w,\theta,\phi), \tag{3}$$

where r_w is the shell minor radius. Note that even though ψ is continuous across the shell, in general, its radial derivative is discontinuous.

In the thin shell limit the eddy currents induced in the shell have no significant radial variation. Consequently, the radially integrated eddy current density can be written as

$$\mu_0\delta\mathbf{I}_w=\nabla\wedge(J_w\hat{\mathbf{r}})\equiv\nabla J_w\wedge\hat{\mathbf{r}}, \tag{4}$$

where $J_w(\theta,\phi)$ is the eddy current stream function. It is helpful to define the quantity

$$\Delta\Psi_w(\theta,\phi)=\left[r\,\frac{\partial\psi(r,\theta,\phi)}{\partial r}\right]_{r_{w-}}^{r_{w+}}, \tag{5}$$

which parametrizes the jump in the radial derivative of ψ across the shell. The nonuniform ''time constant'' of the shell is defined as

$$\tau_w(\theta,\phi)=\mu_0 r_w\sigma_w\delta_w, \tag{6}$$

where $\sigma_w(\theta,\phi)$ and $\delta_w(\theta,\phi)$ are the shell electrical conductivity and radial thickness, respectively.

C. Basic physics

Ampère's law radially integrated across the shell yields

$$\Delta\Psi_w=\frac{\partial J_w}{\partial\theta} \tag{7}$$

in the large aspect-ratio tokamak limit. Ohm's law combined with Faraday's law gives

$$r_w^2\nabla\cdot\left(\frac{1}{\gamma\tau_w}\,\nabla J_w\right)=\frac{\partial\Psi_w}{\partial\theta}, \tag{8}$$

where all perturbed quantities are assumed to vary with time like $\exp(\gamma t)$.

Fourier transformation of the perturbed poloidal flux yields

$$\psi(r,\theta,\phi)=\sum_{m,n}\Psi^{m,n}(r)\exp[i(m\theta-n\phi)]. \tag{9}$$

In the large aspect-ratio tokamak limit, characterized by [see Eq. (2)]

$$|m|\gg|n|\,\epsilon_w, \tag{10}$$

where $\epsilon_w=r_w/R_0\ll1$, the function $\Psi^{m,n}(r)$ obeys the ''cylindrical tearing mode equation,''[39]

$$\frac{1}{r}\frac{d}{dr}\left(r\,\frac{d\Psi^{m,n}}{dr}\right)-\frac{m^2}{r^2}\,\Psi^{m,n}+\frac{\mu_0 J_\phi'}{B_\theta(nq/m-1)}\,\Psi^{m,n}=0. \tag{11}$$

Here, $\mathbf{B}=[0,B_\theta(r),B_\phi]$ is the equilibrium magnetic field, $q(r)=rB_\phi/R_0B_\theta$ is the ''safety factor,'' and $J_\phi'\equiv dJ_\phi/dr$ is the radial gradient of the equilibrium ''toroidal'' plasma current, $\mu_0J_\phi(r)=(1/r)d(rB_\theta)/dr$. The cylindrical tearing mode equation is basically the perturbed force balance equation for an inviscid, massless, perfectly conducting fluid. The large aspect-ratio, low-β, tokamak ordering requires that $B_\theta/B_\phi\ll1$ and also that $q\sim O(1)$. The safety factor is a convenient measure of the helical pitch of the equilibrium magnetic field lines.

Equation (11) is manifestly singular at any ''rational flux surface,'' for which $q=m/n$, except when such surfaces are situated in the vacuum region outside the plasma (where $J_\phi=0$). An acceptable solution of Eq. (11) must satisfy physical boundary conditions at $r=0$ and $r=\infty$, with $\Psi^{m,n}$ continuous across the shell. In addition, $\Psi^{m,n}$ must be zero at any rational surface lying inside the plasma. The latter constraint comes about because modes which interact strongly with the shell tend to be very slowly rotating in the laboratory frame and, therefore, do not reconnect magnetic flux inside the plasma, which is usually rotating substantially faster than the rate of resistive reconnection.[24] In general, there is a discontinuity in the radial derivative of $\Psi^{m,n}$ at $r=r_w$. The parameter

$$\Delta_w^{m,n}=\left[r\,\frac{d\Psi^{m,n}}{dr}\Big/\,\Psi^{m,n}\right]_{r_{w-}}^{r_{w+}} \tag{12}$$

can be uniquely defined for every m,n pair, except for those involving $m=0$. The $m=0$ harmonic is a special case because the inequality (10) is not satisfied for this poloidal harmonic, so the usual large aspect-ratio tokamak approximations break down.

It is helpful to Fourier transform the shell flux $\Psi_w(\theta,\phi)$ and the function $\Delta\Psi_w(\theta,\phi)$:

$$\Psi_w(\theta,\phi)=\sum_{m,n}\Psi_w^{m,n}\exp[i(m\theta-n\phi)], \tag{13a}$$

$$\Delta\Psi_w(\theta,\phi)=\sum_{m,n}\Delta\Psi_w^{m,n}\exp[i(m\theta-n\phi)]. \tag{13b}$$

Thus, from Eq. (12),

$$\Delta_w^{m,n}=\Delta\Psi_w^{m,n}/\Psi_w^{m,n}. \tag{14}$$

It follows from Eq. (7) that

$$\Delta\Psi_w^{m,n}=\Delta_w^{m,n}\Psi_w^{m,n}=imJ_w^{m,n}. \tag{15}$$

D. The resistive shell mode

Consider the simple case in which the time constant τ_w of the shell, as defined by Eq. (6), is uniform. In this situation, Eq. (8) can be Fourier transformed to give

$$imJ_w^{m,n}=\gamma\tau_w\Psi_w^{m,n}, \tag{16}$$

where $O(n\epsilon_w)$ terms have been neglected with respect to $O(m)$ terms, in accordance with the inequality (10). Equation (16) can be combined with Eq. (15) to give a dispersion relation for the m,n mode:

$$\gamma\tau_w=\Delta_w^{m,n}. \tag{17}$$

According to this dispersion relation, a *nonrotating* mode, growing on the characteristic time constant of the shell, becomes unstable whenever the parameter $\Delta_w^{m,n}$ is positive. This instability is usually termed the resistive shell mode,

and $\Delta_w^{m,n}$ is called the ''shell stability index'' for the m,n mode. Recall that $\Delta_w^{m,n}$ is determined by solving the ordinary differential equation (11) subject to suitable boundary conditions. In general, for physically plausible plasma current profiles, at most *one* of the $\Delta_w^{m,n}$ is positive at any given time.[40] Suppose that $\Delta_w^{m_0,n_0}>0$, with $\Delta_w^{m,n}<0$ for $m\neq m_0$ and $n\neq n_0$. Here, m_0,n_0 is termed the ''central harmonic.'' In the presence of a *complete* shell of time constant τ_w the m_0,n_0 resistive shell mode is unstable with growth rate

$$\gamma\tau_w=\Delta_w^{m_0,n_0}, \tag{18}$$

and all other resistive shell modes are stable.

In the vacuum region outside the plasma the perturbed poloidal flux eigenfunction for the central harmonic can be written as

$$\psi(r,\theta,\phi)=\left[\left(1+\frac{\gamma\tau_w}{2|m_0|}\right)\hat{\psi}_{\rm plasma}(r)-\frac{\gamma\tau_w}{2|m_0|}\,\hat{\psi}_{\rm shell}(r)\right]\exp[i(m_0\theta-n_0\phi)], \tag{19}$$

where the Fourier amplitude $\Psi_w^{m_0,n_0}$ is normalized to unity. Here,

$$\hat{\psi}_{\rm plasma}(r)=\left(\frac{r}{r_w}\right)^{-|m_0|} \tag{20}$$

represents that part of the radial eigenfunction which is maintained by plasma currents, and

$$\hat{\psi}_{\rm shell}(r)=\begin{cases}(r/r_w)^{+|m_0|} & \text{for } r<r_w\\ (r/r_w)^{-|m_0|} & \text{for } r\geqslant r_w\end{cases} \tag{21}$$

represents that part which is maintained by eddy currents flowing in the shell.

E. A simple model for a partial shell

Consider, now, the more complicated situation in which the plasma is surrounded by a *partial shell*. Suppose, for the sake of simplicity, that the thickness and conductivity of the metal parts of the shell are uniform. This implies that $\tau_w(\theta,\phi)$ is a constant ($\widetilde{\tau}_w$, say) over the metal parts of the shell, but is zero in the vacuum gaps.

It is possible to formulate a very simplistic model which describes the stability of the m_0,n_0 resistive shell mode in the presence of a partial shell. Suppose that, in the immediate vicinity of the shell, the perturbed poloidal flux at angular coordinates corresponding to *conducting* sections of the shell has an analogous form to that for a complete shell. Hence [see Eq. (19)],

$$\psi(\text{metal})=\left[\left(1+\frac{\gamma\widetilde{\tau}_w}{2|m_0|}\right)\hat{\psi}_{\rm plasma}(r)-\frac{\gamma\widetilde{\tau}_w}{2|m_0|}\,\hat{\psi}_{\rm shell}(r)\right]\exp[i(m_0\theta-n_0\phi)]. \tag{22}$$

Suppose, further, that the perturbed poloidal flux at angular coordinates corresponding to *vacuum gaps* in the shell has an analogous form to that for a complete shell, except that the part which is generated by eddy currents flowing in the shell is missing (since there are no eddy currents flowing in the vacuum gaps). Hence [see Eq. (19)],

$$\psi(\text{gap})=\left[\left(1+\frac{\gamma\widetilde{\tau}_w}{2|m_0|}\right)\hat{\psi}_{\rm plasma}(r)\right]\exp[i(m_0\theta-n_0\phi)]. \tag{23}$$

The m,n harmonic of the perturbed poloidal flux is given by

$$\Psi^{m,n}(r)=\oint\oint\psi(r,\theta,\phi)\exp[-i(m\theta-n\phi)]\,\frac{d\theta}{2\pi}\,\frac{d\phi}{2\pi}. \tag{24}$$

It follows from Eqs. (22) to (24) that

$$\Psi^{m_0,n_0}(r)=\left(1+\frac{\gamma\widetilde{\tau}_w}{2|m_0|}\right)\hat{\psi}_{\rm plasma}(r)-(1-f)\,\frac{\gamma\widetilde{\tau}_w}{2|m_0|}\,\hat{\psi}_{\rm shell}(r), \tag{25}$$

in the immediate vicinity of the shell, where f is the area fraction of vacuum gaps in the shell. According to Eqs. (3), (5), (13), (20), and (21),

$$\Psi_w^{m_0,n_0}=1+f\,\frac{\gamma\widetilde{\tau}_w}{2|m_0|}, \tag{26a}$$

$$\Delta\Psi_w^{m_0,n_0}=(1-f)\,\gamma\widetilde{\tau}_w. \tag{26b}$$

The dispersion relation is obtained via Eq. (15):

$$\gamma\tau_w=\frac{\Delta_w^{m_0,n_0}}{1-\Delta_w^{m_0,n_0}/\Delta_c^{m_0,n_0}}, \tag{27}$$

where

$$\tau_w=(1-f)\,\widetilde{\tau}_w, \tag{28}$$

and

$$\Delta_c^{m_0,n_0}=2|m_0|\left(\frac{1}{f}-1\right). \tag{29}$$

Here, τ_w is the time constant of a uniform shell which contains the same amount of metal as the partial shell. It is easily demonstrated from Eqs. (22) and (23) that the ratio of the amplitudes of the perturbed poloidal flux in the metal and gap sections of the shell is given by

$$\frac{\Psi_{\rm gap}}{\Psi_{\rm metal}}=1+\frac{\gamma\widetilde{\tau}_w}{2|m_0|}. \tag{30}$$

Suppose that the shell stability index for the central harmonic, $\Delta_w^{m_0,n_0}$, is gradually increased from a small positive value. Initially, the poloidal flux is evenly distributed over the metal and gap sections of the shell [see Eq. (30)] and the partial shell acts like a uniform shell containing an equal amount of metal (i.e., $\gamma\tau_w\simeq\Delta_w^{m_0,n_0}$). However, as the m_0,n_0 mode becomes more unstable the poloidal flux starts to concentrate in the gap sections of the shell and the growth rate accelerates. Eventually, at a critical shell stability index, $\Delta_c^{m_0,n_0}$, the poloidal flux is entirely concentrated in the gap sections of the shell and the resistive growth rate becomes

infinite. It is easily demonstrated from Newcomb's criterion[27,41] that the m_0,n_0 ideal external kink mode is unstable for $\Delta_w^{m_0,n_0}>\Delta_c^{m_0,n_0}$. Thus, when the shell stability index exceeds the critical value $\Delta_c^{m_0,n_0}$ the mode ''explodes'' through the gaps in the shell with an ideal growth rate.

The dispersion relation (27) can be rewritten as

$$\gamma\widetilde{\tau}_w=\widetilde{\Delta}_w^{m_0,n_0}, \tag{31}$$

where

$$\widetilde{\Delta}_w^{m_0,n_0}=\frac{(\widetilde{r}_w/r_w)^{2|m_0|}\Delta_w^{m_0,n_0}}{1-(\Delta_w^{m_0,n_0}/2|m_0|)[(\widetilde{r}_w/r_w)^{2|m_0|}-1]} \tag{32}$$

is the shell stability index for the m_0,n_0 mode calculated for a shell located at radius

$$\widetilde{r}_w=r_w\left(1+\frac{2|m_0|}{\Delta_c^{m_0,n_0}}\right)^{1/2|m_0|}=r_w\left(\frac{1}{1-f}\right)^{1/2|m_0|}. \tag{33}$$

According to Eq. (31), a partial shell acts like a complete shell whose radius $\widetilde{r}_w$ is somewhat larger than r_w (the actual radius of the shell), and whose time constant is that of the conducting sections of the partial shell. The ideal stability limit corresponds to $\widetilde{\Delta}_w^{m_0,n_0}\to\infty$. Note that the ideal mode escapes through the gaps in the partial shell, so it is not shielded from the region $r>r_w$, as is the case for a complete shell.

F. Discussion

The main results of this section [i.e., Eqs. (27)–(33)] were obtained using a rather heuristic argument. However, for the special case of a shell containing *toroidal gaps* (i.e., gaps which extend over specific ranges of toroidal angle) it is possible to derive the same results via an exact analytic argument.[40] This derivation is only valid in the limit in which the toroidal lengths of all metal and gap sections of the shell are much greater than the poloidal half-wavelength of the mode. Thus, if L_ϕ is the minimum toroidal length of the metal or gap sections then it is necessary that

$$L_\phi\gg\frac{\pi r_w}{|m_0|}. \tag{34}$$

The derivation also makes use of the ''single harmonic approximation,'' in which it is assumed that the shell stability indices for all harmonics, apart from the central harmonic, take their vacuum values, $\Delta_w^{m,n}=-2|m|$. (In fact, the model presented in Sec. II E tacitly assumes that $\Delta_w^{m,n}=-2|m|$ for all harmonics apart from the central harmonic.) Preliminary analysis has suggested that under some circumstances Eqs. (27)–(33) also hold for shells containing gaps of *arbitrary shape*.[42] In Sec. III a more wide-ranging inquiry is made in order to determine to what extent this is the case.

III. SHELLS CONTAINING HELICAL GAPS

A. Introduction

Consider a shell which possesses M,N helical symmetry, so that

$$\tau_w(\theta+2\pi/M,\phi+2\pi/N)=\tau_w(\theta,\phi) \tag{35}$$

for all values of θ and ϕ. It is convenient to define a helical angle

$$\zeta=\theta-\frac{N}{M}\,\phi, \tag{36}$$

and to express shell quantities as functions of (r,ζ,ϕ) instead of (r,θ,ϕ). In addition, shell quantities are assumed to vary with ϕ like $\exp(-in_*\phi)$. Note that n_* is not necessarily an integer, although it must be a rational number. Thus, $\Psi_w=\Psi_w(\zeta)\exp(-in_*\phi)$, $\Delta\Psi_w=\Delta\Psi_w(\zeta)\exp(-in_*\phi)$, and $J_w=J_w(\zeta)\exp(-in_*\phi)$. Equation (35) implies that $\tau_w=\tau_w(\zeta)$.

In terms of the new variables, Ampère's law [Eq. (7)] is written as

$$\Delta\Psi_w=\frac{\partial J_w}{\partial\zeta}, \tag{37}$$

while Eq. (8) becomes

$$\left[1+\left(\epsilon_w\frac{N}{M}\right)^2\right]\frac{\partial}{\partial\zeta}\left(\frac{1}{\gamma\tau_w}\frac{\partial J_w}{\partial\zeta}\right)+in_*\epsilon_w^2\frac{N}{M}\left[\frac{\partial}{\partial\zeta}\left(\frac{J_w}{\gamma\tau_w}\right)+\frac{1}{\gamma\tau_w}\frac{\partial J_w}{\partial\zeta}\right]-\frac{(n_*\epsilon_w)^2}{\gamma\tau_w}J_w=\frac{\partial\Psi_w}{\partial\zeta}. \tag{38}$$

B. Conducting segments and vacuum gaps

Suppose that at any given toroidal angle ϕ the shell consists of M conducting segments of uniform time constant $\widetilde{\tau}_w$ separated by vacuum gaps. Let the kth segment extend from θ_{k-} to θ_{k+}, where

$$\theta_{k\pm}=\frac{2\pi(k-1)}{M}\pm\frac{\Delta\theta}{2}+\frac{N}{M}\,\phi \tag{39}$$

for $k=1$ to M. Of course, $\Delta\theta<2\pi/M$. In (ζ,ϕ) space the kth segment lies at constant ζ, and extends from ζ_{k-} to ζ_{k+}, where

$$\zeta_{k\pm}=\frac{2\pi(k-1)}{M}\pm\frac{\Delta\theta}{2} \tag{40}$$

for $k=1$ to M.

Now, from Eq. (4),

$$\mu_0\delta\mathbf{I}_w=-i\,\frac{n_*}{R_0}\,J_w\hat{\boldsymbol{\theta}}-\frac{1}{r}\,\frac{\partial J_w}{\partial\zeta}\,\boldsymbol{\phi}_*, \tag{41}$$

where the vector

$$\boldsymbol{\phi}_*=\hat{\boldsymbol{\phi}}+\epsilon_w\frac{N}{M}\,\hat{\boldsymbol{\theta}} \tag{42}$$

runs parallel to the edges of the helical segments in (θ,ϕ) space.

It follows from Eq. (41) that $\partial J_w/\partial\zeta$ is zero in the vacuum gaps, since no eddy currents can flow in these regions. Furthermore, if $n_*\neq0$, then J_w must also be zero in the gaps. However, if $n_*=0$, then this constraint does not apply, and J_w is merely required to be constant in the vacuum gaps. The essential distinction between the $n_*=0$

case and the $n_* \neq 0$ case is obvious from Eq. (41). In the former case, the eddy currents flow parallel to the edges of the helical segments which make up the shell. In the latter case, the currents flow at an angle to the edges of the helical segments. Thus, in the former case it is possible for the eddy currents to flow in a unidirectional continuous loop around each helical segment of the shell, whereas in the latter case this is impossible because the helicity of the currents does not match that of the shell segments. A shell for which $n_* = 0$ is termed a ''resonant shell.'' Likewise, a shell for which $n_* \neq 0$ is termed a ''nonresonant shell.''

C. Nonresonant shells

In the large aspect tokamak limit, characterized by the inequality (10), with the additional constraint

$$|M| \gg |N| \epsilon_w, \tag{43}$$

Eq. (38) yields

$$\frac{\partial J_w}{\partial \zeta} = \gamma \tilde{\tau}_w \begin{cases} \Psi_w + c_k & \zeta_{k-} \leq \zeta \leq \zeta_{k+} \\ 0, & \text{otherwise} \end{cases}, \tag{44}$$

for $k = 1$ to M. Here, the c_k are constants. Consider a nonresonant shell, for which $n_* \neq 0$, and J_w is consequently zero in the vacuum gaps. In this case,

$$\mu_0 I_{\phi k}(\phi) = \int_{\zeta_{k-}}^{\zeta_{k+}} \mu_0 \delta \mathbf{I}_w \cdot \hat{\boldsymbol{\phi}}\ r_w\ d\zeta = [J_w(\zeta_{k-}) - J(\zeta_{k+})] \exp(-i n_* \phi) = 0, \tag{45}$$

since $J_w(\zeta)$ is a continuous function. Here, $I_{\phi k}(\phi)$ is the net toroidal current flowing in the kth conducting segment of the shell at toroidal angle ϕ. It is clear that zero net toroidal current flows in each helical segment of the shell. This is true at all toroidal angles. Equations (44) and (45) can be combined to give

$$\frac{\partial J_w}{\partial \zeta} = \gamma \tilde{\tau}_w \begin{cases} \Psi_w - \int_{\zeta_{k-}}^{\zeta_{k+}} \Psi_w(\zeta') \frac{d\zeta'}{\Delta\theta}, & \zeta_{k-} \leq \zeta \leq \zeta_{k+} \\ 0, & \text{otherwise} \end{cases} \tag{46}$$

for $k = 1$ to M.

Let

$$\Psi_w(\zeta, \phi) = \sum_m \Psi_w^{m;n_*} e^{i(m\zeta - n_* \phi)}, \tag{47a}$$

$$\Delta\Psi_w(\zeta, \phi) = \sum_m \Delta\Psi_w^{m;n_*} e^{i(m\zeta - n_* \phi)}, \tag{47b}$$

$$J_w(\zeta, \phi) = \sum_m J_w^{m;n_*} e^{i(m\zeta - n_* \phi)}, \tag{47c}$$

where m is the conventional poloidal mode number, and n_* is related to the conventional toroidal mode number n via

$$n_* = n - m \frac{N}{M}. \tag{48}$$

By analogy with Eq. (14),

$$\Delta_w^{m;n_*} = \Delta\Psi_w^{m;n_*} / \Psi_w^{m;n_*}. \tag{49}$$

It follows from Eq. (37) that

$$\Delta_w^{m;n_*} \Psi_w^{m;n_*} = i m J_w^{m;n_*}. \tag{50}$$

Equation (46) yields

$$i m J_w^{m;n_*} = \oint \frac{\partial J_w}{\partial \zeta} e^{-im\zeta} \frac{d\zeta}{2\pi} = \gamma \tilde{\tau}_w \frac{M \Delta\theta}{2\pi} \sum_j F(m, m + jM) \Psi_w^{m+jM;n_*}, \tag{51}$$

where

$$F(m, m') = \mathrm{sinc}[(m - m')\Delta\theta/2] - \mathrm{sinc}(m\Delta\theta/2)\mathrm{sinc}(m'\Delta\theta/2), \tag{52}$$

and $\mathrm{sinc}\, x \equiv \sin x / x$. Here, use has been made of Eq. (40).

Note that $F(m, m') = 0$ when $m = 0$ or $m' = 0$. This implies that the $0; n_*$ harmonic completely decouples from the problem. In fact, the value of $\Psi_w^{0;n_*}$ is arbitrary. However, it is convenient to adopt the convention

$$\oint h(\zeta) \Psi_w(\zeta) d\zeta = 0, \tag{53}$$

where

$$h(\zeta) = \begin{cases} 1, & \zeta_{k-} \leq \zeta \leq \zeta_{k+} \\ 0, & \text{otherwise} \end{cases} \tag{54}$$

for $k = 1$ to M. It follows from Eq. (40) that

$$\Psi_w^{0;n_*} = -\sum_{j \neq 0} \mathrm{sinc}(jM\Delta\theta/2) \Psi_w^{jM;n_*}. \tag{55}$$

Integration of Eq. (38) over all values of ζ yields

$$\oint [1 - h(\zeta)] J_w(\zeta) d\zeta = 0, \tag{56}$$

assuming that $n_* \neq 0$. It follows that

$$J_w^{0;n_*} = \frac{M\Delta\theta/2\pi}{1 - M\Delta\theta/2\pi} \sum_{j \neq 0} \mathrm{sinc}(jM\Delta\theta/2) J_w^{jM;n_*}. \tag{57}$$

D. Resonant shells

Consider a resonant shell, for which $n_* = 0$, and J_w is consequently constant in the vacuum gaps. In principle, J_w can take a different value in each gap. It follows from Eq. (45) that

$$\mu_0 I_{\phi k}(\phi) = [J_w(\zeta_{k-}) - J_w(\zeta_{k+})] \neq 0. \tag{58}$$

Thus, a nonzero, constant (in ϕ), toroidal current flows in each helical segment of the shell. However, as is easily demonstrated by summing the above expression from $k = 1$ to N and making use of the fact that $J_w(\zeta)$ is a single-valued function, the total toroidal current flowing in the shell is zero at all toroidal angles, i.e.,

$$\sum_{k=1,N} I_{\phi k}(\phi) = 0. \tag{59}$$

Clearly, in a resonant shell the constraint that zero net toroidal current must flow in each segment of the shell is relaxed to the far less stringent constraint that zero net toroidal current must flow in the shell as a whole. By analogy with Eq. (46), this implies

$$\frac{\partial J_w}{\partial \zeta} = -\gamma \widetilde{\tau}_w \begin{cases} \Psi_w - \oint h(\zeta')\Psi_w(\zeta')\,\dfrac{d\zeta'}{M\Delta\theta}, & \zeta_{k-} \leqslant \zeta \leqslant \zeta_{k+} \\ 0, \quad \text{otherwise} \end{cases} \tag{60}$$

for $k=1$ to M. It follows that

$$imJ_w^{m;0} = \gamma \widetilde{\tau}_w \frac{M\Delta\theta}{2\pi} \sum_j F(m, m+jM)\Psi_w^{m+jM;0}, \tag{61}$$

where

$$F(m,m') = \mathrm{sinc}[(m-m')\Delta\theta/2] \tag{62}$$

provided that $m \neq jM$. Here, j is an integer. If $m=jM$, then $F(m,m')$ is again given by Eq. (52). Note that the 0;0 harmonic decouples from the problem. In fact, the values of $\Psi_w^{0;0}$ and $J_w^{0;0}$ are arbitrary, but are conveniently fixed by adopting the conventions (53) and (56), in which case $\Psi_w^{0;0}$ and $J_w^{0;0}$ are determined by Eqs. (55) and (57), respectively (with $n_* = 0$).

E. Reduction to a matrix eigenvalue problem

Equations (50)–(52), (61) and (62) yield the following dispersion relation for the resistive shell mode:

$$\Delta_w^{m_0,n_0}\ \Psi_w^{m_0,n_0} = \gamma\tau_w \sum_j F(m_0, m_0+jM)\Psi_w^{m_0+jM,n_0+jN}, \tag{63}$$

where j is an integer, and the ''equivalent time constant''

$$\tau_w = \frac{M\Delta\theta}{2\pi}\widetilde{\tau}_w = (1-f\,)\widetilde{\tau}_w \tag{64}$$

is the time constant of a uniform shell of radius r_w which contains the same amount of metal as the segmented shell. The fraction of gaps in the shell is given by

$$f = 1 - \frac{M\Delta\theta}{2\pi}. \tag{65}$$

Note that the above dispersion relation is written in terms of conventional poloidal and toroidal mode numbers, $m=m_0+jM$ and $n=n_0+jN$, respectively. Recall that the central harmonic m_0,n_0 is the only intrinsically unstable harmonic; i.e., the only harmonic for which $\Delta_w^{m_0,n_0} > 0$. Thus, a positive growth rate is only possible when the dispersion relation couples to the central harmonic. The function $F(m,m')$ is given by Eq. (62) for shells which resonate with the central harmonic, i.e., shells which satisfy

$$n_0 M - m_0 N = 0. \tag{66}$$

For shells which do not resonate with the central harmonic (or resonant shells for which $m=jM$) $F(m,m')$ is given by Eq. (52).

The dispersion relation (63) can be written as a matrix eigenvalue problem:

$$(\mathbf{F} - \lambda\boldsymbol{\Delta})\boldsymbol{\Psi}_w = \mathbf{0}, \tag{67}$$

where

$$\lambda = \frac{1}{\gamma\tau_w}, \tag{68}$$

$\boldsymbol{\Psi}_w$ is the vector of the $\Psi_w^{m_0+jM,n_0+jN}$ values, $\mathbf{F}$ is the matrix of the $F(m_0+jM,m_0+kM)$ values, and $\boldsymbol{\Delta}$ is the diagonal matrix of the $\Delta_w^{m_0+jM,n_0+jN}$ values. Here, j and k are integers. The fact that $F(m',m)=F(m,m')$ implies that $\mathbf{F}$ is Hermitian, and hence that λ and γ are real quantities. The nonzero Fourier harmonics of the eddy current stream function are given by

$$J_w^{m_0+jM,n_0+jN} = -i\,\frac{\Delta_w^{m_0+jM,n_0+jN}\Psi_w^{m_0+jM,n_0+jN}}{m_0+jM}, \tag{69}$$

where j is an integer.

For the special case $m_0 = lM$, where l is an integer, the 0, $n_0 - lN$ harmonic couples into the eigenvalue problem. Note that Ψ_w^{0,n_0-lN} is not determined by the solution to Eq. (67), since $F(0,m_0+kM)=F(m_0+jM,0)=0$. Furthermore, J_w^{0,n_0-lN} is not determined by Eq. (69), which is invalid for $m=0$. However, Eqs. (55) and (57) yield

$$\Psi_w^{0,n_0-lN} = -\sum_{j\neq 0} \mathrm{sinc}(jM\Delta\theta/2)\Psi_w^{jM,n_0+(j-l)N}, \tag{70}$$

and

$$J_w^{0,n_0-lN} = \left(\frac{1}{f}-1\right)\sum_{j\neq 0} \mathrm{sinc}(jM\Delta\theta/2)J_w^{jM,n_0+(j-l)N}, \tag{71}$$

respectively.

In principle, $\mathbf{F}$ is an infinite dimensional square matrix. In practice, $\mathbf{F}$ can be approximated as a large, but finite, dimensional square matrix without unduly affecting the physically significant eigenvalues of Eq. (67). This is equivalent to the neglect of high mode number harmonics in the eigenvalue problem.

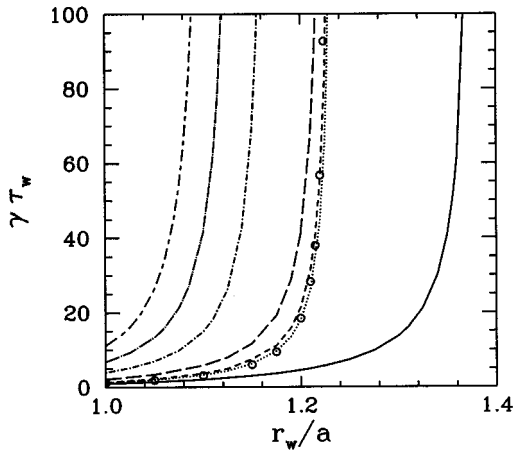

FIG. 1. The growth rate γ of the resistive shell mode plotted as a function of the shell radius r_w for a plasma equilibrium characterized by $q_0=1.3$ and $q_a=2.9$. Data are shown for seven shells with the same equivalent time constant τ_w. The solid curve shows the growth rate for a uniform shell. The other curves show the growth rate for axisymmetric partial shells made up of uniform, identical, and equally spaced (in θ) conducting segments whose total angular extent (in θ) is 180°. The number of segments are one (dotted curve), two (short-dashed curve), three (long-dashed curve), four (dot short-dashed curve), five (dot long-dashed curve), and six (short-dashed, long-dashed curve). The open circles show the growth-rate predicted by the analytic formula (27) for $f=0.5$.

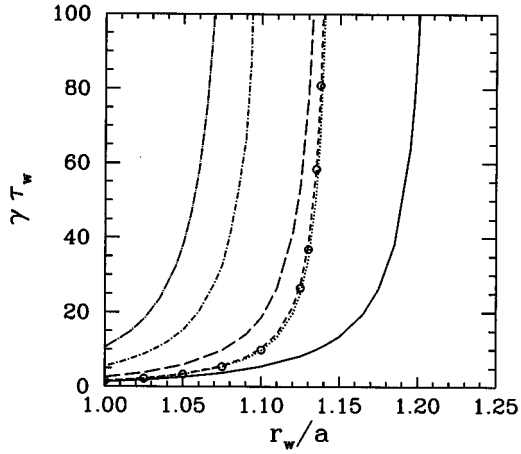

FIG. 2. The growth rate γ of the resistive shell mode plotted as a function of the shell radius r_w for a plasma equilibrium characterized by $q_0=2.92$ and $q_a=5.98$. Data are shown for six shells with the same equivalent time constant τ_w. The solid curve shows the growth rate for a uniform shell. The other curves show the growth rate for axisymmetric partial shells made up of uniform, identical, and equally spaced (in θ) conducting segments whose total angular extent (in θ) is 180°. The number of segments are one (dotted curve), three (short-dashed curve), six (long-dashed curve), nine (dot short-dashed curve), and twelve (dot long-dashed curve). The open circles show the growth rate predicted by the analytic formula (27) for $f=0.5$.

F. Numerical results

1. Wesson profiles

The matrix eigenvalue problem described above has been solved numerically using a ''Wesson-like'' plasma current profile,[39]

$$J_\phi(r)=J_\phi(0)\begin{cases}(1-r^2/a^2)^{q_a/q_0-1}, & r\leqslant a\\ 0, & r>a,\end{cases} \tag{72}$$

where a is the minor radius of the plasma. The associated safety factor profile takes the form

$$q(r)=q_a\begin{cases}\dfrac{r^2/a^2}{1-(1-r^2/a^2)^{q_a/q_0}}, & r\leqslant a\\ r^2/a^2, & r>a\end{cases}. \tag{73}$$

Here, q_0 and q_a are the values of the safety factor on the magnetic axis and at the plasma boundary, respectively. Sufficient helical harmonics are included in the calculation to determine the growth rate of the resistive shell mode to an accuracy of less than 1%. Typically, this requires about 160 harmonics.

2. Axisymmetric shells

In axisymmetric shells (i.e., $N=0$ shells) the conducting segments and the vacuum gaps lie at constant poloidal angle. In this situation, the resonance condition (66) is only satisfied by axisymmetric modes (i.e., $n_0=0$ modes). In fact, such modes are intrinsically stable for the large aspect-ratio, low-β, circular flux surface tokamak equilibria considered in this paper.[39] The intrinsically unstable modes for such equilibria all possess helical symmetry (i.e., $n_0\neq 0$), and do not, therefore, resonate with the shell.

Figure 1 shows the growth rate of the resistive shell mode plotted as a function of the shell radius for a plasma equilibrium characterized by $q_0=1.3$ and $q_a=2.9$. The central harmonic for this equilibrium is $m_0=3$, $n_0=1$, i.e., $\Delta_w^{3,1}>0$, whereas $\Delta_w^{m\neq 3,n\neq 1}<0$. The growth rate is calculated for seven different shells, each of which has the same ''equivalent time constant'' τ_w. The first shell is uniform (i.e., $f=1$). The remainder are axisymmetric partial shells made up of uniform, identical, and equally spaced (in θ) conducting segments whose total angular extent (in θ) is 180° (i.e., $f=0.5$). In other words, the partial shells possess M,0 symmetry, where M is the number of segments. Also shown is the growth rate predicted by the analytic formula (27) for $f=0.5$.

It can be seen that the analytic approximation (27) is in excellent agreement with the exact numerical result for the partial shells consisting of two or less segments. For the shell consisting of three segments the agreement is less impressive. The analytic formula is significantly in error for the shells consisting of more than three segments. Thus, Eq. (27) appears to be a good approximation provided that the poloidal lengths of all metal and gap sections of the shell are greater than the poloidal half-wavelength of the central harmonic, $\pi r_w/|m_0|$. In other words, provided that the angular extents of the metal and gaps sections are greater than 60° (since $m_0=3$ in this case).

Figure 2 shows the growth rate of the resistive shell mode plotted as a function of the shell radius for a plasma equilibrium characterized by $q_0=2.92$ and $q_a=5.98$. The central harmonic for this equilibrium is $m_0=6$, $n_0=1$. The growth rate is calculated for six different shells with the same equivalent time constant τ_w. The first shell is uniform (i.e., $f=1$). The others are axisymmetric partial shells made up of uniform, identical, and equally spaced (in θ) conducting segments whose total angular extent (in θ) is 180° (i.e.,

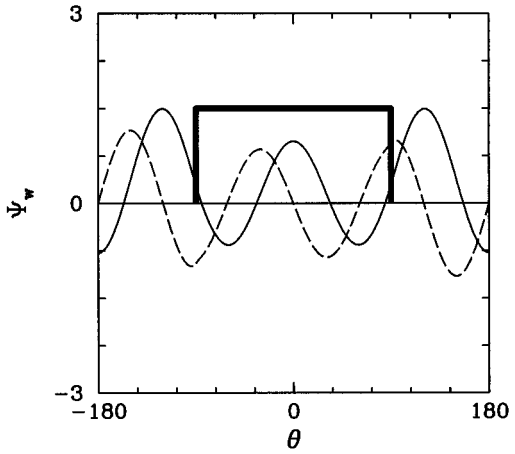

FIG. 3. The shell flux Ψ_w evaluated as a function of the poloidal angle θ for an axisymmetric partial shell of radius $r_w/a=1$. The plasma equilibrium is characterized by $q_0=1.3$ and $q_a=2.9$. The solid and dashed curves show the flux evaluated at two toroidal locations 90° apart (in ϕ). The heavy curve indicates the position of the conducting segment of the shell.

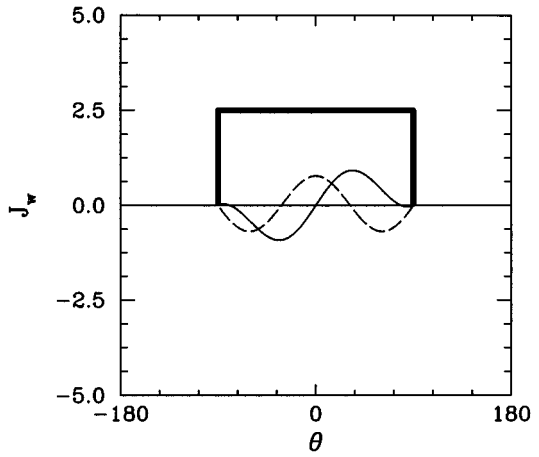

FIG. 4. The eddy current stream function J_w evaluated as a function of the poloidal angle θ for an axisymmetric partial shell of radius $r_w/a=1$. The plasma equilibrium is characterized by $q_0=1.3$ and $q_a=2.9$. The solid and dashed curves show the stream function evaluated at two toroidal locations 90° apart (in ϕ). The heavy curve indicates the position of the conducting segment of the shell.

$f=0.5$). Thus, the partial shells again possess $M,0$ symmetry, where M is the number of segments. Also shown is the growth rate predicted by the analytic formula (27) for $f=0.5$.

The analytic formula is in excellent agreement with the exact numerical result for the partial shells consisting of three or less segments. For the shell consisting of six segments the agreement is not as good. The analytic formula is a poor approximation for the shells consisting of more than six segments. Again, Eq. (27) seems to be valid whenever the poloidal lengths of all metal and gap sections of the shell are greater than the poloidal half-wavelength of the central harmonic. In other words, provided that the angular extents of the metal and gaps sections are greater than 30° (since $m_0=6$ in this case).

Figures 3–6 show the shell flux $\Psi_w(\theta)$ and the eddy current stream function $J_w(\theta)$ evaluated for axisymmetric partial shells located at two different radii. In both cases, the plasma equilibrium is that characterized by $q_0=1.3$ and $q_a=2.9$. The central harmonic for this equilibrium is $m_0=3$, $n_0=1$. The Fourier amplitude $\Psi_w^{3,1}$ is conveniently normalized to unity. Both partial shells consist of a 180° uniform conducting section and a 180° vacuum gap (i.e., both shells possesses 1,0 helical symmetry). It can be seen that when such a shell is situated close to the plasma (i.e., $r_w/a=1$), in which case the 3,1 shell stability index is relatively small (in fact, $\Delta_w^{3,1}=1.010$), the eddy currents induced in the shell are fairly weak and the structure of the mode is not strongly distorted from that of a 3,1 mode. On the other hand, when the same shell is situated further away from the plasma (i.e., $r_w/a=1.22$), so that the 3,1 shell stability index becomes relatively large (in fact, $\Delta_w^{3,1}=5.426$), strong eddy currents are induced in the shell and the mode structure deviates markedly from that of a 3,1 mode. It is clear that the eddy currents tend to expel magnetic flux from the conducting sections of the shell, forcing the flux to concentrate in the vacuum gaps. In fact, for $r_w/a \gtrsim 1.235$ the flux is completely excluded from the conducting sections of the shell, and the mode ''explodes'' through the vacuum gaps with an ideal growth rate. Note that the behavior shown in Figs. 3–6 is exactly that predicted by the simple analytic model introduced in Sec. II E.

3. Resonant shells

According to Eq. (66), a resonant shell satisfies $M,N=\mu(m_0,n_0)$, where μ is a rational number. For $n_0=1$ modes, which are generally the most unstable modes in conventional tokamak plasmas, the only allowed values of μ are the positive integers 1,2,3,... .

Consider the case $\mu=1$, for which $M,N=m_0,n_0$. This a special case, because one of the harmonics which couples into the problem [see Eq. (63)] is the $-m_0,-n_0$ harmonic, i.e., the harmonic with the opposite helicity to the central

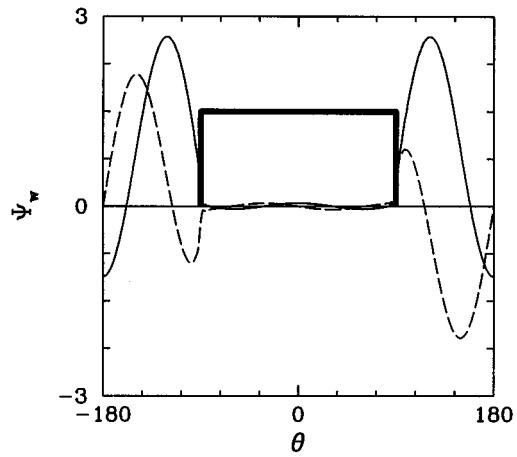

FIG. 5. The shell flux Ψ_w evaluated as a function of the poloidal angle θ for an axisymmetric partial shell of radius $r_w/a=1.22$. The plasma equilibrium is characterized by $q_0=1.3$ and $q_a=2.9$. The solid and dashed curves show the flux evaluated at two toroidal locations 90° apart (in ϕ). The heavy curve indicates the position of the conducting segment of the shell.

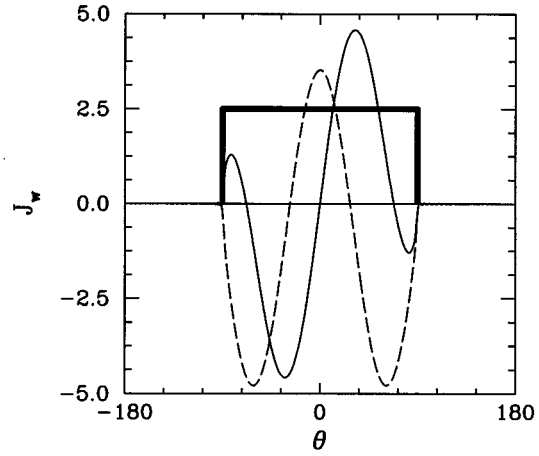

FIG. 6. The eddy current stream function J_w evaluated as a function of the poloidal angle θ for an axisymmetric partial shell of radius $r_w/a=1.22$. The plasma equilibrium is characterized by $q_0=1.3$ and $q_a=2.9$. The solid and dashed curves show the stream function evaluated at two toroidal locations 90° apart (in ϕ). The heavy curve indicates the position of the conducting segment of the shell.

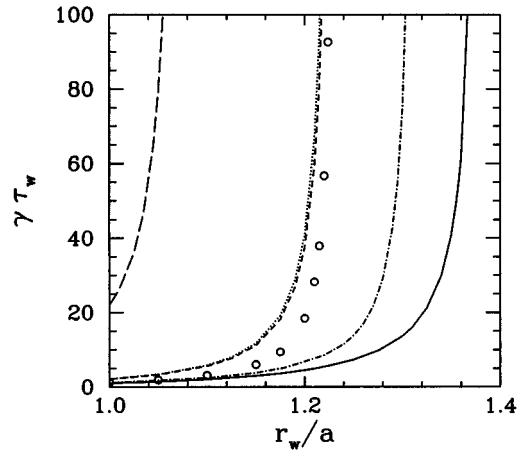

FIG. 7. The growth rate γ of the resistive shell mode plotted as a function of the shell radius r_w for a plasma equilibrium characterized by $q_0=1.3$ and $q_a=2.9$. Data are shown for four shells with the same equivalent time constant τ_w. The solid curve shows the growth rate for a uniform shell. The other curves show the growth rate for partial shells containing three equally spaced helical gaps whose total angular extent (in ζ) is 180°. The various curves correspond to a 3,0 shell (dotted curve), a 3,2 shell (short-dashed curve), and a 3,1 shell. For the latter shell, there are two independent modes; the even mode (long-dashed curve) and the odd mode (dot short-dashed curve). The open circles show the growth rate predicted by the analytic formula (27) for $f=0.5$.

harmonic. Note that the cylindrical tearing mode equation (11) is invariant under the transformation $m,n\rightarrow -m,-n$. This implies that $\Delta_w^{-m_0,-n_0}=\Delta_w^{m_0,n_0}$. In other words, instead of their being a single intrinsically unstable harmonic (i.e., the m_0,n_0 harmonic) in the problem, there are now *two* intrinsically unstable harmonics, albeit with identical positive stability indices, $\Delta_w^{m_0,n_0}$. This allows the growth rate of the resistive shell mode to depend on the *phase* of the mode with respect to the shell. In fact, for a shell which couples the m_0,n_0 harmonic to the $-m_0,-n_0$ harmonic (i.e., any resonant shell for which $2m_0=jM$, where j is an integer), a general resistive shell mode is a linear superposition of *two* independent modes with *different* growth rates; an ''even mode'' [i.e., a mode for which $\Psi_w(\zeta)$ is even (in ζ) across each helical segment of the shell, whereas $J_w(\zeta)$ is odd], and an ''odd mode'' [i.e., a mode for which $\Psi_w(\zeta)$ is odd (in ζ) across each helical segment of the shell, whereas $J_w(\zeta)$ is even]. For a shell which does not couple the m_0,n_0 harmonic to the $-m_0,-n_0$ harmonic, a general resistive shell mode is a linear combination of two independent modes with exactly the same growth rate (see Figs. 3–6).

Figure 7 shows the growth rate of the resistive shell mode plotted as a function of the shell radius for a plasma equilibrium characterized by $q_0=1.3$ and $q_a=2.9$. The central harmonic for this equilibrium is $m_0=3$, $n_0=1$. The growth rate is calculated for four different shells, each of which has the same equivalent time constant τ_w. The first shell is uniform (i.e., $f=1$). The remainder are partial shells containing *three* evenly spaced helical gaps whose total angular extent (in ζ) is 180° (i.e., $f=0.5$). In other words, the partial shells possess 3,*N* symmetry. Also shown is the growth rate predicted by the analytic formula (27) for $f=0.5$.

It can be seen that for the case of the two nonresonant partial shells (i.e., the 3,0 and the 3,2 shells) the growth rate of the resistive shell mode agrees with that described in Sec. III F 2. In other words, since the poloidal lengths of the metal and gap sections of both shells are the same as the poloidal half-wavelength of the central harmonic, the growth rate is in good, but not excellent, agreement with the analytic approximation (27). On the other hand, for the case of the resonant partial shell (i.e., the 3,1 shell) the growth rate of the resistive shell mode deviates markedly from that described in Sec. III F 2. As mentioned above, there are, in fact, two growth rates associated with the 3,1 shell. The growth rate of the ''odd mode'' is markedly less than that predicted by the analytic approximation (27), whereas the growth rate of the ''even mode'' is much greater than that predicted by Eq. (27). Of course, the growth rate of a general resistive shell mode quickly asymptotes to that of the even mode. Thus, it is clear that a $\mu=1$ resonant shell is *less effective* at moderating the growth of an external kink mode than a similar nonresonant shell possessing the same area fraction of gaps. Note that there is zero net toroidal current flowing in each shell segment for both even and odd modes.

Consider the case $\mu=2$, for which $M,N=2(m_0,n_0)$. This is also a special case in which the $-m_0,-n_0$ harmonic couples into the problem. Thus, there are again two independent resistive shell modes (the even mode and the odd mode) with different growth rates.

Figure 8 shows the growth rate of the resistive shell mode plotted as a function of the shell radius for a plasma equilibrium characterized by $q_0=1.3$ and $q_a=2.9$. The central harmonic for this equilibrium is $m_0=3$, $n_0=1$. The growth rate is calculated for four different shells, each of which has the same equivalent time constant τ_w. The first shell is uniform (i.e., $f=1$). The remainder are partial shells containing *six* evenly spaced helical gaps whose total angular extent (in ζ) is 180° (i.e., $f=0.5$). In other words, the partial shells possess 6, *N* symmetry. Also shown is the growth rate

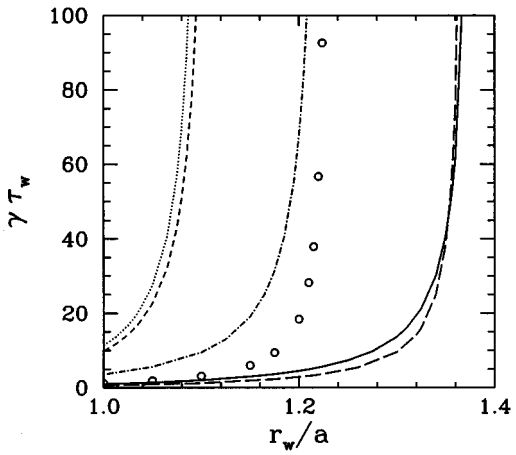

FIG. 8. The growth rate γ of the resistive shell mode plotted as a function of the shell radius r_w for a plasma equilibrium characterized by $q_0=1.3$ and $q_a=2.9$. Data are shown for four shells with the same equivalent time constant τ_w. The solid curve shows the growth rate for a uniform shell. The other curves show the growth rate for partial shells containing six equally spaced helical gaps whose total angular extent (in ζ) is 180°. The various curves correspond to a 6,1 shell (dotted curve), a 6,3 shell (short-dashed curve), and a 6,2 shell. For the latter shell, there are two independent modes; the even mode (long-dashed curve) and the odd mode (dot short-dashed curve). The open circles show the growth rate predicted by the analytic formula (27) for $f=0.5$.

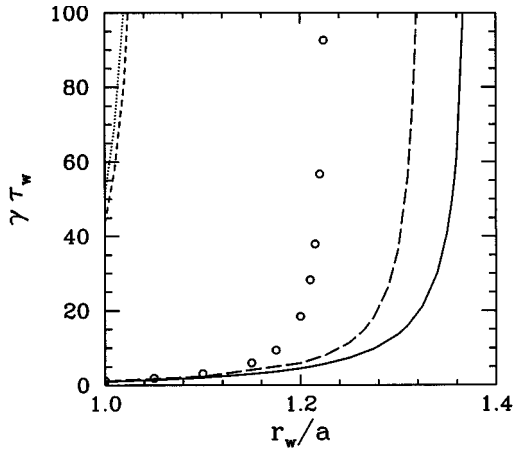

FIG. 9. The growth rate γ of the resistive shell mode plotted as a function of the shell radius r_w for a plasma equilibrium characterized by $q_0=1.3$ and $q_a=2.9$. Data are shown for four shells with the same equivalent time constant τ_w. The solid curve shows the growth rate for a uniform shell. The other curves show the growth rate for partial shells containing nine equally spaced helical gaps whose total angular extent (in ζ) is 180°. The various curves correspond to a 9,2 shell (dotted curve), a 9,3 shell (long-dashed curve), and a 9,4 shell (short-dashed curve). The open circles show the growth-rate predicted by the analytic formula (27) for $f=0.5$.

predicted by the analytic formula (27) for $f=0.5$.

For the case of the two nonresonant shells (i.e., the 6,1 and 6,3 shells) the growth rate of the resistive shell mode again agrees with that described in Sec. III F 2. That is, since the poloidal lengths of the metal and gap sections of both shells are less than the poloidal half-wavelength of the central harmonic, the growth rate is significantly greater than that predicted by the analytic approximation (27). For the case of the resonant partial shell (i.e., the 6,2 shell), the growth rate of the odd mode is slightly larger than that predicted by Eq. (27), whereas the growth rate of the even mode is virtually the same as that obtained for a uniform shell. Of course, the growth rate of a general resistive shell mode quickly asymptotes to that of the odd mode. Thus, it is clear that a $\mu=2$ resonant shell is *more effective* at moderating the growth of an external kink mode than a similar nonresonant shell possessing the same area fraction of gaps. Note that there is zero net toroidal current flowing in each shell segment for the odd mode, whereas nonzero currents of alternating direction flow in the segments for the even mode.

Consider, finally, the case $\mu=3$. The $-m_0$, $-n_0$ harmonic does not couple into the problem in this case, so the growth rate of the resistive shell mode does not depend on the phase of the mode with respect to the shell.

Figure 9 shows the growth rate of the resistive shell mode plotted as a function of the shell radius for a plasma equilibrium characterized by $q_0=1.3$ and $q_a=2.9$. The central harmonic for this equilibrium is $m_0=3$, $n_0=1$. The growth rate is calculated for four different shells, each of which has the same equivalent time constant τ_w. The first shell is uniform (i.e., $f=1$). The remainder are partial shells containing *nine* evenly spaced helical gaps whose total angular extent (in ζ) is 180° (i.e., $f=0.5$). In other words, the partial shells possess 9, N symmetry. Also shown is the growth rate predicted by the analytic formula (27) for $f=0.5$.

For the case of the two nonresonant shells (i.e., the 9,2 and 9,4 shells) the growth rate of the resistive shell mode again agrees with that described in Sec. III F 2. That is, since the poloidal lengths of the metal and gap sections of both shells are much less than the poloidal half-wavelength of the central harmonic, the growth rate is very much greater than that predicted by the analytic approximation (27). For the case of the resonant partial shell (i.e., the 9,3 shell), the growth rate of the resistive shell mode is slightly larger than that obtained for a uniform shell. Thus, it is clear that a $\mu=3$ resonant shell is *far more effective* at moderating the growth of an external kink mode than a similar nonresonant shell possessing the same area fraction of gaps. Note that a nonzero toroidal current flows in each helical segment for the case of a $\mu=3$ resonant shell, whereas zero net current flows in each segment for the case of a nonresonant shell.

For $\mu>3$, the growth rate of the resistive shell mode behaves in an analogous manner to that shown in Fig. 9. As μ increases, the growth rate asymptotes to that of a uniform shell possessing the same equivalent time constant, τ_w: the growth rate for a similar nonresonant shell asymptotes to infinity.

The above results were obtained by considering a particular plasma equilibrium whose central harmonic is $m_0=3$, $n_0=1$. These results are, nevertheless, quite general, as can easily be verified by considering other plasma equilibria with different central harmonics.

Consider the limit $f\to 1$, in which the angular extents of the helical shell segments tend to zero. In this limit, the growth rate of the resistive shell mode tends to infinity for all nonresonant shells. The situation is somewhat more complicated for resonant shells. For $\mu=1$, the growth rate of both

the even and odd modes tend to infinity. For $\mu=2$, the growth rate of the odd mode tends to infinity, whereas the growth rate of the even mode asymptotes to that obtained for a complete shell with the same equivalent time constant. Finally, for $\mu>2$ the growth rate of the resistive shell mode asymptotes to that obtained for a complete shell with the same equivalent time constant. Thus, in the limit $f\rightarrow 1$ there is a very marked difference in the ability of a nonresonant and a $\mu>2$ resonant shell to moderate the growth of an external kink mode. In the former case, the shell is quite incapable of moderating the growth of the mode, whereas in the latter case the shell performs almost as well as a complete (i.e., $f=1$) shell possessing the same equivalent time-constant.

G. Summary

In parametrizing the ability of a partial shell made up of M,N helical conducting segments to moderate the growth of an m_0,n_0 external kink mode, it is necessary to make a distinction between *resonant* and *nonresonant* shells. In the former case it is possible for m_0,n_0 eddy currents to flow in unidirectional continuous loops around each helical segment of the shell, whereas in the latter case this is impossible because the helicity of the segments does not match that of the kink mode. Thus, in the former case a nonzero toroidal current can, in principle, flow in each helical segment of the shell, whereas in the latter case zero net toroidal current flows in each segment. Of course, in both cases zero net toroidal current flows in the shell, as a whole, at any given toroidal location.

For the case of a nonresonant shell the analytic model presented in Sec. II E very successfully accounts for both the growth rate and the structure of the resistive shell mode, provided that the poloidal extents of all metal and gap sections of the shell exceed the poloidal half-wavelength of the mode, $\pi r_w/|m_0|$. In Ref. 40 it is demonstrated that the analytic model also works for shells containing toroidal gaps, provided that the toroidal extents of all metal and gap sections of the shell exceed the poloidal half-wavelength of the mode. Thus, it is reasonable to assume that the model described in Sec. II E also holds for shells containing gaps of arbitrary shape (see Ref. 42), provided that the dimensions of all metal and gap sections exceed the poloidal half-wavelength of the central harmonic, and also that the gaps are such as to prevent m_0, n_0 eddy currents from flowing in unidirectional continuous loops around the shell.

Resonant shells satisfy $m_0,n_0=\mu(M,N)$, where $\mu=1,2,3,...$ for $n_0=1$ modes (which are, typically, the most unstable modes in tokamaks). For $\mu=1$, the eddy currents excited in the shell couple the $-m_0,-n_0$, and m_0,n_0 harmonics. Consequently, the growth rate of the resistive shell mode depends on the phase of the mode with respect to the shell. The most unstable mode, the so-called even mode, is such that the perturbed radial magnetic field peaks at the center of the gaps at all toroidal angles. The growth rate of this mode is far larger than that obtained for a similar nonresonant shell containing the same area fraction of gaps. Thus, $\mu=1$ resonant shells are less able to moderate the growth of an external kink mode than similar nonresonant shells. For $\mu=2$, the shell again couples the $-m_0,-n_0$, and m_0,n_0 harmonics. The most unstable resistive shell mode, the so-called odd mode, is again such that the perturbed radial magnetic field peaks at the center of the gaps at all toroidal angles. The growth rate of this mode is somewhat less than that obtained for a similar nonresonant shell containing the same area fraction of gaps. Thus, $\mu=2$ resonant shells are better able to moderate the growth of an external kink mode than similar nonresonant shells. For $\mu>2$ resonant shells, the growth rate of the resistive shell mode is independent of the phase of the mode with respect to the shell. In fact, the growth rate is almost identical to that obtained for a complete shell possessing the same equivalent time constant. On the other hand, for similar nonresonant shells the growth rate of the mode greatly exceeds that obtained for an equivalent complete shell. Thus, $\mu>2$ resonant shells are far better able to moderate the growth of an external kink mode than similar nonresonant shells.

IV. SKELETAL SHELLS

A. Introduction

The most striking conclusion of the previous section is that which pertains to skeletal (i.e., $f\rightarrow 1$) shells. It is found that nonresonant skeletal shells are virtually incapable of moderating the growth of the ideal external kink mode, whereas ($\mu>2$) resonant skeletal shells perform almost as well as complete shells possessing the same equivalent time constant. In order to more clearly understand this rather surprising phenomenon, this section is devoted to an investigation of the ability of skeletal shells constructed from thin helical wires (whose mutual spacing is much greater than their diameter) to moderate the growth of the ideal external kink mode.

B. Preliminary analysis

Consider a set of M uniform z-directed wires of diameter d. Suppose that the kth wire carries a current I_k and is located at position vector $\mathbf{r}_k$ in (x,y) space. It is assumed that the typical spacing between the wires, b, is much greater than d. The magnetic field generated by the currents flowing in the wires is given by $\mathbf{B}_{\rm wires}=\nabla\psi_{\rm wires}\wedge\hat{\mathbf{z}}$, where

$$\psi_{\rm wires}(\mathbf{r})=-\frac{\mu_0}{2\pi}\sum_{k=1,M} I_k\,\ln|\mathbf{r}-\mathbf{r}_k|. \tag{74}$$

The energy per unit length contained in the magnetic field distribution is

$$W=\frac{1}{2}\sum_{k=1,M} L_k I_k^2+\frac{1}{2}\sum_{k,l=1,M}^{k\neq l} M_{kl}\;I_k I_l, \tag{75}$$

where L_k is the self-inductance per unit length of the kth wire, and M_{kl} is the mutual inductance per unit length between the kth and lth wires. Assuming that the wires carry zero net current, i.e.,

$$\sum_{k=1,M} I_k=0, \tag{76}$$

the self- and mutual inductances can be easily shown to take the form

$$L_k=\frac{\mu_0}{2\pi}\left[g-\ln\frac{d}{2}+O\left(\frac{d}{b}\right)\right], \tag{77a}$$

$$M_{kl}=\frac{\mu_0}{2\pi}\left[-\ln|\mathbf{r}_k-\mathbf{r}_l|O\left(\frac{d}{b}\right)\right], \tag{77b}$$

where

$$g(\xi)=\int_0^1\left|\frac{I_1(\xi y)}{I_1(\xi)}\right|^2 y\,dy. \tag{78}$$

Here, I_1 is a standard Bessel function, $\xi=\sqrt{\gamma\mu_0/\pi R}$, and R is the resistance per unit length of the wires. It is assumed that all fields and currents vary in time like $\exp(\gamma t)$. Note that

$$g(\xi)\to\begin{cases}1/4 & \text{as } \xi\to 0\\ 1/(2|\xi|) & \text{as } \xi\to\infty.\end{cases} \tag{79}$$

The circuit equation for the kth wire is

$$-\gamma\psi_{\rm ext}(\mathbf{r}_k)-\gamma L_k I_k-\gamma\sum_{l=1,M}^{l\neq k} M_{kl}I_l=RI_k, \tag{80}$$

where $\mathbf{B}_{\rm ext}=\nabla\psi_{\rm ext}\wedge\hat{\mathbf{z}}$ is the magnetic field generated by currents external to the region containing the wires. The external field is also assumed to vary in time like ext(γt). The total magnetic field is given by $\mathbf{B}=\nabla\psi\wedge\hat{\mathbf{z}}$, where

$$\psi(\mathbf{r})=\psi_{\rm ext}(\mathbf{r})-\frac{\mu_0}{2\pi}\sum_{k=1,M} I_k\,\ln|\mathbf{r}-\mathbf{r}_k|. \tag{81}$$

C. Resonant skeletal shells

1. Analysis

Consider the kink stability of a tokamak plasma surrounded by a skeletal shell of minor radius r_w which is constructed out of helical wires. Suppose that at any given toroidal angle ϕ there are M wires located at poloidal angles

$$\theta_k=\frac{2\pi(k-1)}{M}+\frac{N}{M}\,\phi, \tag{82}$$

for $k=1$ to M. Clearly, the shell possesses M,N helical symmetry. It is convenient to adopt the single harmonic approximation,

$$\Delta_w^{m/n}=-2|m| \tag{83}$$

for $m,\ n\neq m_0,\ n_0$, with $\Delta_w^{m_0,n_0}>0$. Thus, the shell stability indices for all harmonics, apart from the intrinsically unstable central harmonic, take their vacuum values (i.e., the values obtained in the absence of the plasma). It is assumed that the shell is resonant, so that $M,N=\mu(m_0,n_0)$. It follows that, in principle, a nonzero current I_k is able to flow in the kth wire. Recall, from Sec. III, that if the shell is nonresonant then zero net current must flow in each wire. In the large aspect-ratio limit, the wires at any given toroidal location are directed essentially in the ϕ (or z) direction. Thus, the results of Sec. IV B can be applied to this problem.

The external perturbed poloidal magnetic flux (i.e., the flux generated by perturbed currents flowing in the plasma) at the shell is given by

$$\psi_{\rm ext}(r_w,\theta,\phi)=\sum_{m,n}^{m\neq 0}\left(1+\frac{\Delta_w^{m/n}}{2|m|}\right)\Psi_w^{m/n}\times\exp[i(m\theta-n\phi)]. \tag{84}$$

Moreover, application of Ampère's law yields

$$\Delta\Psi_w^{m_0,n_0}=\Delta_w^{m_0,n_0}\Psi_w^{m_0,n_0}=-\frac{\mu_0}{2\pi}\sum_{k=1,M} I_k e^{-im_0\zeta_k}, \tag{85}$$

where $\zeta_k=2\pi(k-1)/M$.

Suppose that

$$I_k=\hat{I}e^{im_0\zeta_k} \tag{86}$$

for $k=1$ to M, where $\hat{I}$ is a constant. According to Eq. (76), the total current carried by the wires at any given toroidal angle must be zero. This is the case provided that $m_0\neq jM$, where j is an integer. It follows from Eqs. (82) to (86) that

$$\psi_{\rm ext}(\mathbf{r}_k)=-\frac{\mu_0}{2\pi}\left(1+\frac{\Delta_w^{m_0,n_0}}{2|m_0|}\right)\frac{M\hat{I}e^{im_0\zeta_k}}{\Delta_w^{m_0,n_0}} \tag{87}$$

for $k=1$ to M. Thus, the circuit equation for the kth wire reduces to

$$\gamma\left(1+\frac{\Delta_w^{m_0,n_0}}{2|m_0|}\right)\frac{M}{\Delta_w^{m_0,n_0}}-\gamma\hat{L}_k-\gamma\sum_{l=1,M}^{l\neq k}\hat{M}_{kl}e^{im_0(\zeta_l-\zeta_k)}=\frac{2\pi R}{\mu_0}, \tag{88}$$

where $L_k=(\mu_0/2\pi)\hat{L}_k$ and $M_{kl}=(\mu_0/2\pi)\hat{M}_{kl}$. The above equation can be rearranged to give

$$\gamma\tau_w=\frac{\Delta_w^{m_0,n_0}}{1-\Delta_w^{m_0,n_0}/\Delta_c^{m_0,n_0}}, \tag{89}$$

where

$$\tau_w=\frac{\mu_0 M}{2\pi R} \tag{90}$$

is the equivalent time constant, i.e., the time constant of a uniform shell of minor radius r_w which contains the same amount of metal as the skeletal shell. The quantity $\Delta_c^{m_0,n_0}$ is given by

$$\Delta_c^{m_0,n_0}=\frac{M}{\hat{L}_k+\Sigma_{l=1,M}^{l\neq k}\hat{M}_{kl}e^{im_0(\zeta_l-\zeta_k)}-M/(2|m_0|)}. \tag{91}$$

It follows from Eqs. (76) and (77) that

$$\frac{M}{\Delta_c^{m_0,n_0}}=g(\sqrt{2\gamma\tau_w/M})+\ln(4r_w/d)-\sum_{l=1,M}^{l\neq k}\ln[\sin(\pi|l-k|/M)]e^{i2\pi(l-k)m_0/M}-M/(2|m_0|), \tag{92}$$

since $|\mathbf{r}_k-\mathbf{r}_l|=2r_w\sin(|\zeta_k-\zeta_l|/2)$, which yields

$$\Delta_c^{m_0,n_0}=\frac{M}{g(\sqrt{2\gamma\tau_w/M})+\ln(2r_w/Md)+K(M,|m_0|)} \tag{93}$$

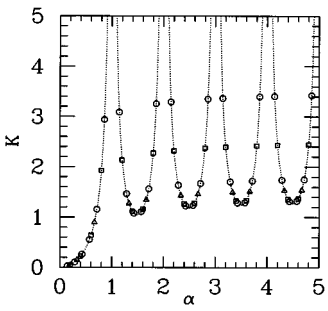

FIG. 10. The function $K(M,|m_0|)$ plotted against $\alpha=|m_0|/M$. Data are not shown for the cases where α is an integer, since the expression (93) is not valid in this situation. The triangular, square, and circular points correspond to $M=3$, 5, and 7, respectively. The dotted curve shows the function $K_0(\alpha)$.

for all values of k, where

$$K(M,|m_0|)=\ln(2M)-\frac{M}{2|m_0|}-\sum_{j=1,M-1}\ln[\sin(\pi j/M)]\cos(2\pi j/|m_0|/M). \tag{94}$$

The fact that the value of $\Delta_c^{m_0,n_0}$ given by Eq. (91) is independent of the value of k suggests that the initial guess (86) for the distribution of currents flowing in the wires is correct. In the limit that $M\to\infty$ the function $K(M,|m_0|)$ reduces to

$$K_0(\alpha)=\ln(2\pi)-\frac{1}{2\alpha}+\sum_{j=1}^{\infty}\frac{\sin[\pi(2j+1)\alpha]}{\sin(\pi\alpha)}\times\ln\left(1+\frac{1}{j}\right), \tag{95}$$

where $\alpha=|m_0|/M$.

Figure 10 shows $K(M,|m_0|)$ and $K_0(|m_0|/M)$ plotted as functions of $|m_0|/M$. It can be seen that $K(M,|m_0|)=K_0(|m_0|/M)$. In other words, the two functions are identical. This only ceases to be the case when $m_0=jM$, where j is an integer. However, in this situation the expression (93) is invalid. It follows that Eq. (93) can be written in the simplified form

$$\Delta_c^{m_0,n_0}=\frac{M}{g(\sqrt{2\gamma\tau_w/M})+\ln(2r_w/Md)+K_0(|m_0|/M)}. \tag{96}$$

Equations (76), (81), (83), (84), (85), and (86) give

$$\Psi_w(\zeta)=\left(1+\frac{\Delta_w^{m_0,n_0}}{2|m_0|}\right)\Psi_w^{m_0,n_0}e^{im_0\zeta}+\frac{\Delta_w^{m_0,n_0}\Psi_w^{m_0,n_0}}{M}\times\sum_{k=1,M}\ln[\sin(|\zeta_k-\zeta|/2)]e^{im_0\zeta_k}, \tag{97}$$

where $\zeta=\theta-(N/M)\phi$. Let

$$f(\zeta)=\frac{\Psi_w(\zeta)}{\Psi_w^{m_0,n_0}e^{im_0\zeta}}. \tag{98}$$

It is clear that the function $f(\zeta)$ is periodic; i.e.,

$$f(\zeta+2\pi j/M)=f(\zeta), \tag{99}$$

where j is an integer. Let

$$\zeta=\frac{2\pi s}{M}, \tag{100}$$

for $0\leqslant s\leqslant 1$. It is easily demonstrated that

$$f(s)=1-\frac{\Delta_w^{m_0,n_0}}{\Delta_{c\infty}^{m_0,n_0}}\,h(s), \tag{101}$$

where

$$\Delta_{c\infty}^{m_0,n_0}=\lim_{\gamma\to\infty}\Delta_c^{m_0,n_0}=\frac{M}{\ln(2r_w/Md)+K_0(|m_0|/M)}, \tag{102}$$

and

$$h(s)=\frac{\Sigma_{j=0,M-1}\ln[\sin(\pi|j-s|/M)]e^{i2\pi(j-s)|m_0|/M}+M/(2|m_0|)}{\ln(\pi s_w/M)+\Sigma_{j=1,M-1}\ln[\sin(\pi j/M)]\cos(2\pi j|m_0|/M)+M/(2|m_0|)}. \tag{103}$$

Here,

$$s_w=\frac{Md}{4\pi r_w}\ll 1 \tag{104}$$

is the normalized helical coordinate of the edge of a wire, as is $1-s_w$. Equation (101) is only valid in the vacuum region $s_w\leqslant s\leqslant 1-s_w$. Note that $\mathrm{Re}[h(1-s)]=\mathrm{Re}[h(s)]$, whereas $\mathrm{Im}[h(1-s)]=-\mathrm{Im}[h(s)]$. It can be seen that $h(s_w)=h(1-s_w)\simeq 1$. It follows from Eqs. (98) and (101) that

$$\left|\frac{\Psi_{w\ \mathrm{wires}}}{\Psi_w^{m_0,n_0}}\right|=1-\frac{\Delta_w^{m_0,n_0}}{\Delta_{c\infty}^{m_0,n_0}}, \tag{105}$$

where $\Psi_{w\ \mathrm{wires}}$ is the perturbed poloidal flux at the edges of the wires. Note that $\mathrm{Re}[h(s)]\sim\mathrm{Im}[h(s)]$ when $M\sim O(1)$, but that $\mathrm{Im}[h(s)]/\mathrm{Re}[h(s)]\to 0$ as $M\to\infty$.

Figure 11 shows the normalized amplitude of the shell flux f plotted as a function of the normalized helical angle s for a case where $s_w=0.01$. It can be seen that when the shell stability index for the central harmonic $\Delta_w^{m_0,n_0}$ is much less than the critical value $\Delta_{c\infty}^{m_0,n_0}$, $f(s)$ is uniform. However, as the ratio $\Delta_w^{m_0,n_0}/\Delta_{c\infty}^{m_0,n_0}$ increases, magnetic flux is gradually expelled from the wires, in accordance with Eq. (105), and accumulates in the vacuum gaps between the wires. Eventually, when $\Delta_w^{m_0,n_0}=\Delta_{c\infty}^{m_0,n_0}$, there is no magnetic flux left in

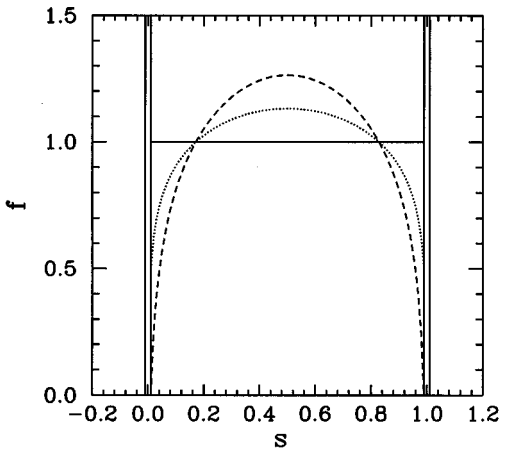

FIG. 11. The normalized amplitude of the shell flux f plotted as a function of the normalized helical angle s for three different values of $\Delta_w^{m_0,n_0}/\Delta_{c\infty}^{m_0,n_0}$. Two of the wires which make up the shell are shown (at $s=0$ and $s=1$). The angular diameter of the wires is 0.02 normalized units. The function $f(s)$ is plotted in the region between the two wires for $M=12$ and $m_0=3$. The solid curve corresponds to $\Delta_w^{m_0,n_0}/\Delta_{c\infty}^{m_0,n_0}=0$, the dotted curve corresponds to $\Delta_w^{m_0,n_0}/\Delta_{c\infty}^{m_0,n_0}=0.5$, and the dashed curve corresponds to $\Delta_w^{m_0,n_0}/\Delta_{c\infty}^{m_0,n_0}=1$.

the wires. At this point, the growth rate of the resistive shell mode becomes infinite [see Eq. (89)].

2. Discussion

The growth rate of the resistive shell mode for the case of a resonant skeletal shell constructed from helical wires is determined by Eq. (89). Note that this expression is similar to the dispersion relation (27) obtained in Sec. II E, except that the form of the parameter $\Delta_c^{m_0,n_0}$ is different. As was demonstrated in Sec. III, the simple analytic model outlined in Sec. II E successfully accounts for the properties of the resistive shell mode for nonresonant shells, provided that the dimensions of all metal and gap sections exceed the poloidal half-wavelength of the central harmonic. It can now be seen that the analytic model of Sec. II E can also be applied to resonant skeletal shells [where, by definition, the length of the metal sections of the shell (i.e., the wires) in one direction is much less than the poloidal half-wavelength of the central harmonic], provided that the critical shell stability index $\Delta_c^{m_0,n_0}$ is determined by Eq. (96), instead of Eq. (29). Note that $\Delta_c^{m_0,n_0}$ is a weak function of the growth rate γ via the function $g(\gamma)$, which determines the amount of magnetic flux penetrating into the interior of the wires. When the growth rate is relatively large (i.e., $\gamma\tau_w \gg M$) $\Delta_c^{m_0,n_0}(\gamma)$ asymptotes to the constant value $\Delta_{c\infty}^{m_0,n_0}$ [see Eq. (102)]. The dispersion relation (89) can be interpreted in exactly the same manner as the earlier dispersion relation (27). When the shell stability index for the central harmonic $\Delta_w^{m_0,n_0}$ is much less than its critical value $\Delta_{c\infty}^{m_0,n_0}$, the amplitude of the magnetic flux in the wires is equal to that in the vacuum gaps, and the growth rate of the resistive shell mode is the same as that obtained for a uniform shell containing the same amount of metal as the wires. However, as $\Delta_w^{m_0,n_0}$ approaches $\Delta_{c\infty}^{m_0,n_0}$, magnetic flux is gradually expelled from the wires [see Eq. (105) and Fig. 11], and the growth rate of the resistive shell mode accelerates. Finally, when the shell stability index reaches the critical value $\Delta_{c\infty}^{m_0,n_0}$ [defined by Eq. (102)] there is no flux remaining in the wires, and the growth rate of the resistive shell mode becomes infinite: this corresponds to the marginal stability point for the m_0,n_0 ideal external kink mode. For $\Delta_w^{m_0,n_0} > \Delta_{c\infty}^{m_0,n_0}$ the mode explodes between the wires with an ideal growth-rate.

According to Eq. (102) and Fig. 10, the critical shell stability index $\Delta_{c\infty}^{m_0,n_0}$ is zero whenever $|m_0|=jM$, where j is a nonzero integer. In other words, an M,N resonant skeletal shell is quite incapable of moderating the growth of the m_0,n_0 external kink mode if $|m_0|$ is a nonzero integer multiple of M. This is not a surprising result. Equation (86) implies that $I_k=\hat{I}$ for all k (i.e., the same current flows in each wire at any given toroidal angle) whenever $|m_0|=jM$. This immediately yields $\hat{I}=0$ (i.e., zero current flows in each wire) since, by symmetry, a helical mode cannot induce a net toroidal current in a passive conducting shell. Thus, the m_0,n_0 mode excites no eddy currents in the shell if $|m_0|$ is a nonzero integer multiple of M, which implies that the shell is unable to affect the growth rate of the mode.

At first sight, Eq. (102) and Fig. 10 seem to suggest that the critical shell stability index $\Delta_{c\infty}^{m_0,n_0}$ takes a particularly large value whenever $|m_0|=(j+1/2)M$, where j is an integer. However, this is not necessarily the case. Equation (86) yields $I_k=|\hat{I}|(-1)^{k-1}$ when $\hat{I}$ is purely real, and $I_k=0$ when $\hat{I}$ is purely imaginary (since the physical current flowing in the kth wire is obtained by taking the real part of I_k). Figure 10 determines the critical shell stability index of the former mode, but not the latter. In fact, the critical shell stability index of the latter mode is zero, since the mode excites no eddy currents in the shell. In other words, when $|m_0|=(j+1/2)M$ the growth rate of the resistive shell mode depends on its phase. It is possible to find a particular phase for which no eddy currents are excited in the shell, and the shell is, therefore, unable to affect the growth rate of the mode. There is a second, linearly independent, phase for which eddy currents of alternating direction are excited in the wires making up the shell: the shell is clearly capable of moderating the growth rate of the mode in this case (in fact, the critical stability index is that determined by Fig. 10).

When $|m_0|\neq jM$ and $|m_0|\neq(j+1/2)M$, where j is an integer, the nonzero critical shell stability index $\Delta_{c\infty}^{m_0,n_0}$ for the m_0,n_0 mode is determined by Eq. (102) and Fig. 10, with no qualifications. In this case, the growth rate of the resistive shell mode is independent of its phase.

It now remains to make a connection between the results of this section and those of Sec. III F 3. The case $|m_0|=jM$, where j is an integer, corresponds to the case $\mu=1$ investigated in Sec. III F 3. Recall, from Sec. III F 3, that in the skeletal limit, $f\rightarrow 1$, the growth rate of the resistive shell mode tends to infinity for a $\mu=1$ resonant shell. Furthermore, zero net toroidal current is excited in each helical segment of the shell. These results are in complete accordance with the results of this section, where it is found that when $|m_0|=jM$ no currents are excited in the helical wires making

up the shell, and the growth rate of the resistive shell mode becomes infinite. The case $|m_0|=(j+1/2)M$, where j is an integer, corresponds to the case $\mu=2$ investigated in Sec. III F 3. Recall, from Sec. III F 3, that in the skeletal limit, $f\rightarrow 1$, the growth rate of the resistive shell mode for a $\mu=2$ resonant shell tends to infinity for one particular phase of the mode, and tends to a finite value in the other linearly independent phase. In the former case, zero net toroidal current is excited in each helical segment of the shell, whereas in the latter case nonzero currents of alternating direction are excited in the segments. These results are, again, in complete accordance with the results of this section, where it is found that when $|m_0|=(j+1/2)M$ there are two linearly independent resistive shell modes. The first mode excites no eddy currents in the helical wires making up the shell and, therefore, has a growth rate which tends to infinity. The second mode excites eddy currents of alternating direction in the wires and possesses a finite growth rate. Finally, the case $|m_0|\neq jM$ and $|m_0|\neq(j+1/2)M$, where j is an integer, corresponds to the case $\mu>2$ investigated in Sec. III F 3. Recall, from Sec. III F 3, that in the skeletal limit, $f\rightarrow 1$, the growth rate of the resistive shell mode remains finite for a $\mu>2$ resonant shell. This accords well with the results of this section, where the growth rate of the resistive shell mode is finite whenever $|m_0|\neq jM$ and $|m_0|\neq(j+1/2)M$. Note, from Eq. (102), that as the number of helical wires M increases, but the area fraction of metal (proportional to Md) remains constant, the critical shell stability index $\Delta_{c\infty}^{m_0,n_0}$ tends to infinity. Thus, in this limit, the skeletal shell acts like a complete shell with the same equivalent time constant. Recall, from Sec. III F 3, that in the analogous limit $\mu\rightarrow\infty$ the shell also acts like a complete shell with the same equivalent time constant.

D. Nonresonant skeletal shells

1. Analysis

A nonresonant partial shell built up from helical conducting segments is subject to the constraint that zero net toroidal current must flow in each segment (see Sec. III). Thus, it is not possible to construct an effective nonresonant shell from independent helical wires, since zero current must flow in each wire, and the shell is, therefore, incapable of moderating the growth of the ideal external kink mode. Consider, instead, a shell of minor radius r_w constructed from M identical wire *loops*, each consisting of two interconnected helical wires. The kth loop is such that the (approximately toroidal) current $I_k(\phi)$ flows at $\theta=\theta_k+\Delta\theta/2$ and the return current $-I_k(\phi)$ flows at $\theta=\theta_k-\Delta\theta/2$, where θ_k is given by Eq. (82), for $k=1$ to M. It is assumed that the two wires which make up the kth loop (located at poloidal angles $\theta_k\pm\Delta\theta/2$) are connected together at a sufficiently large number of toroidal locations that $I_k(\phi)$ is able to vary freely with toroidal angle. In practice, this means that the toroidal spacing of the connections must be less that the toroidal half-wavelength, $\pi R_0/n_0$, of the central harmonic.

By analogy with the analysis of Secs. IV B and IV C, the circuit equation for the kth loop is given by

$$V_k-\gamma L_k I_k-\gamma\sum_{l=1,M}^{l\neq k} M_{kl}I_l=2RI_k, \tag{106}$$

for $k=1$ to M. Here, V_k is the voltage (per unit length) around the kth loop, at $\phi=0$ (say), due to induction by currents flowing external to the shell. Likewise, I_k is the current circulating in the kth loop at $\phi=0$. Furthermore, R is the resistance per unit length of the wires making up the loops, L_k is the self-inductance per unit length of the kth loop, and M_{kl} is the mutual inductance per unit length between the kth and lth loops. Adopting the single harmonic approximation exemplified by Eq. (83), it is easily demonstrated that

$$V_k=-\gamma\left(1+\frac{\Delta_w^{m_0,n_0}}{2|m_0|}\right)\Psi_w^{m_0,n_0}e^{im_0\theta_k}(2i)\sin(m_0\Delta\theta/2). \tag{107}$$

Application of Ampères's law at $\phi=0$ yields

$$\Delta\Psi_w^{m_0,n_0}=\Delta_w^{m_0,n_0}\Psi_w^{m_0,n_0}=-\frac{\mu_0}{2\pi}\sum_{k=1,M}I_k e^{-im_0\theta_k}(-2i)\sin(m_0\Delta\theta/2). \tag{108}$$

Finally, the self- and mutual inductances of the loops are

$$L_k=\frac{\mu_0}{2\pi}\left(2g+2\ln\left[\frac{4r_w\,\sin(\Delta\theta/2)}{d}\right]\right), \tag{109}$$

and

$$M_{kl}=\frac{\mu_0}{2\pi}\ln\left[1-\frac{\sin^2(\Delta\theta/2)}{\sin^2([\theta_k-\theta_l]/2)}\right], \tag{110}$$

respectively, where $g(\xi)$ is given by Eq. (78), and $\xi=\sqrt{2\gamma\mu_0/\pi R}$.

Suppose that at $\phi=0$

$$I_k=\hat{I}e^{im_0\theta_k}, \tag{111}$$

for $k=1$ to M, where $\hat{I}$ is a constant. Note that the currents, $I_k(\phi)$, circulating in the loops, and the voltages (per unit length), $V_k(\phi)$, generated by external induction, vary with toroidal angle like $e^{i(m_0N/M-n_0)\phi}$. Equations (106)–(108) yield the dispersion relation

$$\gamma\tau_w=\frac{\Delta_w^{m_0/n_0}}{1-\Delta_w^{m_0,n_0}/\Delta_c^{m_0,n_0}}, \tag{112}$$

where

$$\tau_w=\sin^2(m_0\Delta\theta/2)\,\overline{\tau_w}, \tag{113}$$

and

$$\Delta_c^{m_0,n_0}=\frac{4\sin^2(m_0\Delta\theta/2)\;\;M}{\hat{L}_k+\Sigma_{l=1,M}^{l\neq k}\hat{M}_{kl}e^{i2\pi(l-k)m_0/M}-4\sin^2(m_0\Delta\theta/2)\;\;M/(2|m_0|)}. \tag{114}$$

Here,

$$\overline{\tau_w}=\frac{\mu_0 M}{\pi R}. \tag{115}$$

is the equivalent time constant of the shell (i.e., the time constant of a uniform shell of radius r_w containing the same amount of metal as the loops), $L_k=(\mu_0/2\pi)\hat{L}_k$, and $M_{kl}=(\mu_0/2\pi)\hat{M}_{kl}$.

Let $\alpha=|m_0|/M$, $\kappa=M\Delta\theta/2\pi$, and $\epsilon=Md/2\pi r_w$. The parameter κ measures the fractional area coverage of the loops, whereas the parameter ϵ measures the fractional area coverage of the wires making up the loops. Geometric arguments easily yield the constraint $\epsilon<\kappa<1-\epsilon$. Equation (114) reduces to

$$\Delta_c^{m_0,n_0}=MF(\gamma,M,\epsilon,\kappa,\alpha), \tag{116}$$

where

$$F=\frac{2\sin^2(\pi\kappa\alpha)}{g(\sqrt{2\gamma\overline{\tau_w}/M})+\ln[2M\;\sin(\pi\kappa/M)/\pi\epsilon]+J(M,\kappa,\alpha)-\sin^2(\pi\kappa\alpha)/\alpha}, \tag{117}$$

and

$$J(M,\kappa,\alpha)=\frac{1}{2}\sum_{j=1,M-1}\ln\left[1-\frac{\sin^2(\pi\kappa/M)}{\sin^2(\pi j/M)}\right]\times\cos(2\pi j\alpha). \tag{118}$$

The fact that the value of $\Delta_c^{m_0,n_0}$ given by Eq. (114) is independent of the value of k suggests that the initial guess (111) for the distribution of currents circulating in the loops at $\phi=0$ is correct. According to the dispersion relation (112), the growth rate of the resistive shell mode tends to infinity as $\Delta_w^{m_0,n_0}\rightarrow\Delta_{c\infty}^{m_0,n_0}$, where

$$\Delta_{c\infty}^{m_0,n_0}=\lim_{\gamma\rightarrow\infty}\Delta_c^{m_0,n_0}. \tag{119}$$

It follows from Eqs. (79) and (116) that

$$\Delta_{c\infty}^{m_0,n_0}=MF_\infty(M,\epsilon,\kappa,\alpha), \tag{120}$$

where

$$F_\infty=\frac{2\sin^2(\pi\kappa\alpha)}{\ln[2M\;\sin(\pi\kappa/M)/\pi\epsilon]+J(M,\kappa,\alpha)-\sin^2(\pi\kappa\alpha)/\alpha}. \tag{121}$$

In the limit $M\rightarrow\infty$,

$$F_\infty\rightarrow G_\infty(\epsilon,\kappa,\alpha)=\frac{2\sin^2(\pi\kappa\alpha)}{\ln(2\kappa/\epsilon)+J_0(\kappa,\alpha)-\sin^2(\pi\kappa\alpha)/\alpha}, \tag{122}$$

where

$$J_0(\kappa,\alpha)=\sum_{j=1,\infty}\ln\left[1-\frac{\kappa^2}{j^2}\right]\cos(2\pi j\alpha). \tag{123}$$

Figures 12, 13, and 14 show F_∞ and G_∞ plotted as functions of α for $\epsilon=0.01$, $\kappa=0.02$, 0.5, and 0.98, respectively, and various values of M. In all cases, it can be seen that

$$F_\infty(M,\epsilon,\kappa,\alpha)=G_\infty(\epsilon,\kappa,\alpha). \tag{124}$$

This strongly suggests that, in general,

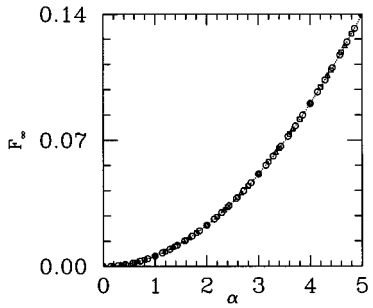

FIG. 12. The function $F_\infty(M,\epsilon,\kappa,\alpha)$ plotted against $\alpha=|m_0|/M$ for $\epsilon=0.01$, $\kappa=0.02$, and various integer values of m_0. The triangular, square, and circular points correspond to $M=3$, 5, and 7, respectively. The dotted curve shows the function $G_\infty(\epsilon,\kappa,\alpha)$.

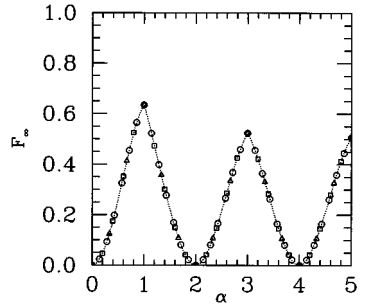

FIG. 13. The function $F_\infty(M,\epsilon,\kappa,\alpha)$ plotted against $\alpha=|m_0|/M$ for $\epsilon=0.01$, $\kappa=0.5$, and various integer values of m_0. The triangular, square, and circular points correspond to $M=3$, 5, and 7, respectively. The dotted curve shows the function $G_\infty(\epsilon,\kappa,\alpha)$.

$$\Delta_c^{m_0,n_0}$$

$$= \frac{2M\ \sin^2(\pi\kappa\alpha)}{g(\sqrt{2\gamma\overline{\tau_w}/M}) + \ln(2\kappa/\epsilon) + J_0(\kappa,\alpha) - \sin^2(\pi\kappa\alpha)/\alpha}, \tag{125a}$$

$$\Delta_{c\infty}^{m_0,n_0} = \frac{2M\ \sin^2(\pi\kappa\alpha)}{\ln(2\kappa/\epsilon) + J_0(\kappa,\alpha) - \sin^2(\pi\kappa\alpha)/\alpha}. \tag{125b}$$

It is clear from Figs. 12–14 that the critical shell stability index $\Delta_{c\infty}^{m_0,n_0}$ achieves its maximum value when $\kappa\alpha = j + 1/2$, where j is an integer. This corresponds to $|m_0|\Delta\theta/2 = (j+1/2)\pi$. In other words, a nonresonant skeletal shell is best able to moderate the growth of the ideal external kink mode when the poloidal extents of the loops which make up the shell are odd-integer multiples of the poloidal half-wavelength of the central harmonic. In this situation, the time constant of the shell is *equal* to the equivalent time constant, according to Eq. (113). It is also clear from Figs. 12–14 that the critical shell stability index tends to zero when $\kappa\alpha = j$, where j is an integer. This corresponds to $|m_0|\Delta\theta/2 = j\pi$. In other words, a nonresonant skeletal shell is incapable of moderating the growth of the ideal external kink mode when the poloidal extents of the loops which make up the shell are integer multiples of the poloidal wavelength of the central harmonic. In this situation, the time constant of the shell also tends to zero, according to Eq. (113). If $|m_0|\Delta\theta/2$ is neither a half-integer nor an integer multiple of π then the properties of the shell lie somewhere between the two extremes described above. Finally, in the limit in which the poloidal extents of the loops making up the shell are much less than the poloidal half-wavelength of the central harmonic (i.e., $|m_0|\Delta\theta/2 \ll 1$), Eq. (125b) reduces to

$$\Delta_{c\infty}^{m_0,n_0} \simeq \frac{M(|m_0|\Delta\theta)^2}{2\ln(2r_w\Delta\theta/d)}, \tag{126}$$

and Eq. (113) yields

$$\tau_w \cong \frac{(|m_0|\Delta\theta)^2}{4}\,\overline{\tau_w}. \tag{127}$$

Thus, in the limit of narrow loops the critical shell stability index becomes relatively small, and the time constant of the shell becomes much less than the equivalent time constant. Clearly, in this limit the shell is fairly ineffective at moderating the growth of the ideal external kink mode.

2. Discussion

The growth rate of the resistive shell mode for the case of a nonresonant skeletal shell constructed from helical wire loops is determined by Eq. (112). Note that this expression is similar to the dispersion relation (27) obtained in Sec. II E, except that the forms of the parameters τ_w and $\Delta_c^{m_0,n_0}$ are different. Judging from the results of Secs. III and IV, it appears highly likely that the dispersion relation for the resistive shell mode always takes the form (27) in situations where the single harmonic approximation is valid. However, the expressions for the time constant τ_w and critical stability index $\Delta_c^{m_0,n_0}$ clearly depend on the type of shell in question. For the case of a nonresonant shell constructed from helical wire loops the two parameters are determined by Eqs. (113) and (125a), respectively. The critical shell stability index $\Delta_c^{m_0,n_0}$ is again a weak function of the growth rate γ, but asymptotes to the constant value $\Delta_{c\infty}^{m_0,n_0}$ [see Eq. (125b)] as $\gamma\to\infty$. The dispersion relation (112) can be interpreted in the standard manner. When the shell stability index for the central harmonic $\Delta_w^{m_0,n_0}$ is much less than its critical value $\Delta_{c\infty}^{m_0,n_0}$, the mode grows on the time scale τ_w, which, in this case, is less than or equal to the equivalent time constant (i.e., the time constant of a uniform shell of radius r_w containing the same amount of metal as the loops). However, as $\Delta_w^{m_0,n_0}$ approaches $\Delta_{c\infty}^{m_0,n_0}$ the time scale on which the mode grows gradually shortens. Eventually, when the shell stability index reaches the critical value $\Delta_{c\infty}^{m_0,n_0}$ the time scale becomes zero: this corresponds to the marginal stability point for the m_0, n_0 ideal external kink mode. For $\Delta_w^{m_0,n_0} > \Delta_{c\infty}^{m_0,n_0}$ the mode explodes through the loops with an ideal growth-rate.

It now remains to make a connection between the results of this section and those of Secs. III F 2 and III F 3. In Sec. IV C it was found that the behavior of a *resonant* shell built up from *narrow* (i.e., such that the poloidal extents of the strips are *much smaller* than the poloidal half-wavelength of the central harmonic) helical conducting strips can be accounted for, at a qualitative level, by modeling each strip as a helical *wire* possessing the same helicity and the same resistance per unit length. This model cannot be applied to a similar *nonresonant* shell because of the constraint, which applies to all nonresonant shells, that zero net toroidal current must flow in each strip: this constraint implies that each wire carries zero current, so the model shell has no effect on the growth rate of the ideal resistive shell mode. A more sensible approach is to model each strip as a helical wire *loop* possessing the same helicity and resistance per unit

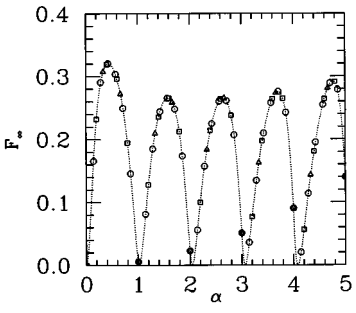

FIG. 14. The function $F_\infty(M,\epsilon,\kappa,\alpha)$ plotted against $\alpha = |m_0|/M$ for $\epsilon = 0.01$, $\kappa = 0.98$, and various integer values of m_0. The triangular, square, and circular points correspond to $M = 3$, 5, and 7, respectively. The dotted curve shows the function $G_\infty(\epsilon,\kappa,\alpha)$.

length. By definition, zero net toroidal current flows in a helical loop, so the above-mentioned constraint does not preclude a nonzero current from circulating in each loop. The dimensions of the loops are determined as follows: the angular width $\Delta\theta$ of the loops is the same as the angular width of the strips, and the diameters of the helical wires making up the loops are the same as the radial thickness of the strips. According to Eqs. (127), the model predicts that the time constant of the shell is $(|m_0|\Delta\theta)^2/4$ times the equivalent time constant. In other words, the time constant is much less than the equivalent time constant (by a factor which is of order the ratio of the poloidal width of the helical strips to the poloidal half-wavelength of the central harmonic, squared). According to Eq. (126), the model predicts that the critical shell stability index is relatively small (the index is proportional to the ratio of the poloidal width of the helical strips to the poloidal half-wavelength of the central harmonic, squared). Clearly, the model suggests that a nonresonant shell built up from *narrow* helical strips is very ineffective at moderating the growth of the ideal external kink mode. This conclusion is entirely consistent with the results of Secs. III F 2 and III F 3.

E. Summary and discussion

The main results of this section are the resistive shell mode dispersion relation (89) for a *resonant* skeletal shell made up of helical wires, and the resistive shell mode dispersion relation (112) for a *nonresonant* skeletal shell made up of helical wire loops. In fact, both these dispersion relations have exactly the same form as the resistive shell mode dispersion relation (27) derived in Sec. II E. Note that all three dispersion relations depend on the single harmonic approximation. The latter dispersion relation is valid for any nonresonant shell for which the dimensions of all metal and gap sections exceed the poloidal half-wavelength of the central harmonic (see Sec. III G). This criterion clearly excludes skeletal shells. The fact that the same dispersion relation is also obtained for both resonant and nonresonant skeletal shells strongly suggests that Eq. (27),

$$\gamma\tau_w=\frac{\Delta_w^{m_0,n_0}}{1-\Delta_w^{m_0,n_0}/\Delta_c^{m_0,n_0}}, \tag{128}$$

represents a *universal* form for the resistive shell mode dispersion relation (provided that the single harmonic approximation is valid). In the above dispersion relation, τ_w is the time constant of the shell, whereas $\Delta_c^{m_0,n_0}$ is the ''critical shell stability index.'' The shell is capable of stabilizing the ideal external kink mode provided that $\Delta_w^{m_0,n_0}<\Delta_c^{m_0,n_0}$. The resistive shell mode is unstable, and grows on the typical time scale τ_w, whenever $0<\Delta_w^{m_0,n_0}\leq\Delta_c^{m_0,n_0}$. As $\Delta_w^{m_0,n_0}$ approaches $\Delta_c^{m_0,n_0}$, the growth rate of the resistive shell mode rises precipitously until it attains that characteristic of the ideal external kink mode. The expressions for the parameters τ_w and $\Delta_c^{m_0,n_0}$ depend on the nature of the shell. For the case of a nonresonant shell for which the dimensions of all metal and gap sections are larger than the poloidal half-wavelength of the central harmonic, τ_w and $\Delta_c^{m_0,n_0}$ are given by Eqs. (28) and (29), respectively. For the case of a resonant skeletal shell constructed from helical wires, τ_w and $\Delta_c^{m_0,n_0}$ are given by Eqs. (90) and (96), respectively. Finally, for the case of a nonresonant skeletal shell constructed from helical wire loops, τ_w and $\Delta_c^{m_0,n_0}$ are given by Eqs. (113) and (125a), respectively.

The analysis of *skeletal* shells is worthwhile for two main reasons. First, it permits a qualitative understanding of the results of Secs. III F 2 and III F 3, which pertain to shells constructed from *narrow* helical conducting strips. It is clear that the marked difference in the ability of $(\mu>2)$ resonant and nonresonant shells to moderate the growth of the ideal external kink mode comes about because in the former case a net toroidal current is able flow in each strip, whereas in the latter case zero net current must flow in each strip (see Sec. III). Thus, resonant shells are similar to skeletal shells constructed from helical wires: the eddy currents excited in the shell flow through the strips in *unidirectional continuous loops*, so the strips act rather like wires. On the other hand, nonresonant shells are similar to skeletal shells constructed from narrow helical wire loops: the eddy currents excited in the shell are forced to *circulate* in the strips, which are narrow, so the strips act rather like narrow wire loops. According to the analysis presented in this section, both the time constant, τ_w, and the critical shell stability index, $\Delta_c^{m_0,n_0}$, are much lower for a nonresonant skeletal shell constructed from narrow helical wire loops than for a $(\mu>2)$ resonant skeletal shell constructed from helical wires. This conclusion is is good agreement with the results of Secs. III F 2 and III F 3. The second main reason for analyzing shells constructed from helical wires and helical wire loops is that such analysis is a necessary prerequisite for evaluating realistic feedback control schemes for the resistive shell mode.

V. APPLICATIONS

A. Introduction

The theory presented in Secs. II–IV has many interesting and important applications in tokamak fusion physics. In this section, a few of these applications are examined in depth.

B. The design of passive stabilizing shells

Consider the stability of the ideal external kink mode for the case of a tokamak plasma surrounded by a *partial* shell of minor radius r_w. It is convenient to adopt the single harmonic approximation, in which the shell stability indices for all harmonics, apart from the central harmonic m_0,n_0, take their vacuum values $-2|m|$. It is easily demonstrated that this is an excellent approximation, unless the shell is located very close to the edge of the plasma.[40] The shell stability index for the central harmonic can always be written in the form

$$\Delta_w^{m_0,n_0}=\frac{2|m_0|}{(r_c/r_w)^{2|m_0|}-1}. \tag{129}$$

Here, r_c is termed the critical radius for the m_0,n_0 ideal external kink mode. A *complete*, perfectly conducting shell

whose radius is less than the critical radius is able to stabilize the ideal external kink mode, whereas a similar shell whose radius is greater than the critical radius is incapable of stabilizing the mode. The resistive shell mode dispersion relation for a complete *resistive* shell takes the form

$$\gamma\tau_w=\Delta_w^{m_0,n_0}, \tag{130}$$

where τ_w is the time constant of the shell. Thus, the resistive shell mode is unstable wherever $\Delta_w^{m_0,n_0}>0$. The growth rate of the resistive shell mode merges with that of the ideal external kink mode as $\Delta_w^{m_0,n_0}\to\infty$. So, the marginal stability point for the latter mode is $1/\Delta_w^{m_0,n_0}=0$. It follows from Eq. (129) that the ideal external kink mode is stable and the resistive shell mode is unstable for $r_w<r_c$, whereas the ideal external kink mode is unstable for $r_w>r_c$.

The resistive shell mode dispersion relation for a *partial* shell takes the general form (see Sec. IV E)

$$\gamma\tau_w=\frac{\Delta_w^{m_0,n_0}}{1-\Delta_w^{m_0,n_0}/\Delta_c^{m_0,n_0}}. \tag{131}$$

Here, τ_w is the time constant of the shell, whereas $\Delta_c^{m_0,n_0}$ is termed the critical shell stability index. The resistive shell mode is unstable whenever $0<\Delta_w^{m_0,n_0}<\Delta_c^{m_0,n_0}$. The growth rate of the resistive shell mode merges with that of the ideal external kink mode as $\Delta_w^{m_0,n_0}\to\Delta_c^{m_0,n_0}$. Thus, the marginal stability point for the latter mode is $\Delta_w^{m_0,n_0}=\Delta_c^{m_0,n_0}$.

Equations (129) and (131) can be combined to give

$$\gamma\widetilde{\tau}_w=\widetilde{\Delta}_w^{m_0,n_0}, \tag{132}$$

where

$$\widetilde{\Delta}_w^{m_0,n_0}=\frac{2|m_0|}{(r_c/\widetilde{r}_w)^{2|m_0|}-1}, \tag{133}$$

with

$$\widetilde{\tau}_w=\tau_w\left(1+\frac{2|m_0|}{\Delta_c^{m_0,n_0}}\right), \tag{134}$$

and

$$\widetilde{r}_w=r_w\left(1+\frac{2|m_0|}{\Delta_c^{m_0,n_0}}\right)^{1/2|m_0|}. \tag{135}$$

It is clear from a comparison of Eqs. (130) and (132) that a *partial* shell of time constant τ_w and radius r_w acts in exactly the same manner as a *complete* shell of effective time constant $\widetilde{\tau}_w$ and effective radius $\widetilde{r}_w$. In other words, it is possible to replace a partial shell by a complete effective shell whose time constant and radius are both *larger* than those of the actual shell. As the radius $\widetilde{r}_w$ of the effective shell approaches the critical radius r_c, the growth rate of the resistive shell mode merges with that of the ideal external kink mode. Thus, the marginal stability criterion for the latter mode corresponds to $\widetilde{r}_w=r_c$. It follows that the ideal external kink mode is stable and the resistive shell mode is unstable for $\widetilde{r}_w<r_c$, whereas the ideal external kink mode is unstable for $\widetilde{r}_w>r_c$.

For the special case of a partial shell in which the extents of all metal and gap sections exceed the poloidal half-wavelength of the central harmonic, $\pi r_w/|m_0|$, and the gaps are such such as to prevent m_0,n_0 eddy currents from flowing in unidirectional continuous loops around the plasma (i.e., the shell is nonresonant), it can be shown that (see Sec. III)

$$\tau_w=(1-f)\,\overline{\tau_w}, \tag{136a}$$

$$\Delta_c^{m_0,n_0}=2|m_0|\left(\frac{1}{f}-1\right), \tag{136b}$$

where f is the area fraction of gaps, and $\overline{\tau_w}=\mu_0 r_w\sigma_w\delta_w$. Here, σ_w and δ_w are the conductivity and (uniform) thickness of the metal sections of the shell, respectively. Incidentally, the value of τ_w given in Eq. (136a) is equal to the equivalent time constant, which is defined as the time constant of a uniform shell of radius r_w which contains the same amount of metal as the partial shell. Equations (134)–(136) yield

$$\widetilde{\tau}_w=\overline{\tau_w}, \tag{137}$$

and

$$\widetilde{r}_w=r_w\left(\frac{1}{1-f}\right)^{1/2|m_0|}. \tag{138}$$

Thus, in this special case, the effective shell possesses the same time constant as the metal sections of the actual shell. As the fraction of gaps is increased, the radius of the effective shell also increases. This implies, not surprisingly, that the shell becomes progressively less capable of stabilizing the ideal external kink mode as the fraction of gaps is made larger.

The results of Secs. III and IV indicate that if a nonresonant partial shell is such that the extents of all metal or gap sections *do not* exceed the poloidal half-wavelength of the central harmonic, $\pi r_w/|m_0|$, then the performance of the shell is worse than that indicated above. In fact, Figs. 1 and 2 clearly suggest that, in this situation, the time constant, τ_w, and the critical shell stability index, $\Delta_c^{m_0,n_0}$, of the shell are both *less* than the values given in Eqs. (136). In particular, the time constant of the shell falls below the equivalent time constant. It follows from Eq. (135) that, in this case, the radius of the effective shell is *larger* than that given in Eq. (138). Thus, a nonresonant partial shell in which the extents of all metal and gap sections exceed the poloidal half-wavelength of the central harmonic is better able to stabilize the ideal external kink mode that a similar shell (i.e., a nonresonant partial shell containing the same amount of metal and the same area fraction of gaps) in which this is not the case. Clearly, it is of great importance, when designing a nonresonant passive stabilizing shell, to ensure that the extents of all metal and gap sections *exceed* the poloidal half-wavelength of the central harmonic.

A partial shell which permits m_0,n_0 eddy currents to flow in unidirectional continuous loops around the plasma is termed a resonant shell. The results of Secs. III and IV indicate that a resonant partial shell which possesses only *one* helical path per helical period of the central harmonic (this

corresponds to the $\mu=1$ case discussed in Sec. III F 3) performs worse than a similar nonresonant shell (i.e., a nonresonant shell containing the same amount of metal and the same area fraction of gaps). The basic reason for this behavior is the existence of a particular phase for the resistive shell mode at which the m_0,n_0 eddy currents excited in the shell divert magnetic flux strongly through the gaps in the shell. The results of Secs. III and IV also indicate that a resonant partial shell which possesses *two* independent helical paths per helical period of the central harmonic (this corresponds to the $\mu=2$ case discussed in Sec. III F 3) performs better than a similar nonresonant shell. Furthermore, a resonant partial shell which possesses *three* or *more* independent helical paths per helical period of the central harmonic (this corresponds to the $\mu>2$ case discussed in Sec. III F 3) performs much better than a similar nonresonant shell: the performance improves as the number of independent paths increases. In fact, the results of Sec. IV C suggest that for a resonant partial shell which possesses three or more independent helical paths per helical period of the central harmonic, the time constant of the shell is equal to the equivalent time constant, and the critical shell stability index tends to infinity as the number of paths tends to infinity. These results are true irrespective of whether the extents of the metal and gap sections of the shell exceed the poloidal half-wavelength of the central harmonic.

The following general conclusions may be drawn regarding the ability of a partial shell to moderate the growth of the ideal external kink mode. For a *nonresonant* shell the optimum performance is achieved when the extents of all metal and gap sections exceed the poloidal half-wavelength of the central harmonic. In this case, the shell acts like an effective complete shell whose time constant is the same as the conducting portions of the actual shell and whose radius is somewhat larger than the radius of the actual shell. Note that the radius of the effective shell, which is given in Eq. (138), only depends on the area fraction of gaps in the actual shell. For a resonant shell the optimum performance is achieved when there are very many (i.e., at least two) independent helical paths through the shell per helical period of the central harmonic. In this case, the shell acts like an effective complete shell whose radius is that of the actual shell, and whose time constant is the same as the equivalent time constant (i.e., the average time constant of the metal and gap sections of the actual shell). Consequently, it is possible to improve the performance of a nonresonant partial shell by installing ''jump leads'' between separate metal sections of the shell, so as to form at least two helical paths in the shell per helical period of the central harmonic. The jump leads have the effect of decreasing the radius of the effective shell, although, somewhat paradoxically, they also decrease its time constant.

C. Feedback stabilization of the resistive shell mode

1. The fake rotating shell concept

The results of Sec. IV, which deals with partial shells constructed from thin helical wires or thin wire loops, can be used to investigate whether feedback stabilization schemes for the resistive shell mode remain feasible when realistic sets of feedback coils are employed. Consider, for example, the recently proposed fake rotating shell stabilization scheme.[43] In the original proposal, the feedback controlled conductors consist of a fine *network* of interconnected toroidal and poloidal wires which completely surrounds the plasma. A separate power amplifier is needed for each cell in the network. The scheme works by mimicking the eddy current pattern of a poloidally rotating resistive shell using the feedback controlled network of conductors. Thus, to all intents and purposes, the network acts like a poloidally *rotating* resistive shell. The combination of a stationary conventional shell (e.g., the vacuum vessel) surrounded by a fake rotating shell (i.e., the feedback controlled network of conductors) is capable of stabilizing the resistive shell mode provided that the effective angular rotation frequency of the fake shell (which is proportional to the gain in the feedback circuits) is greater than the inverse L/R time of the network. In the following, two variants of the original fake rotating shell stabilization scheme which may be easier to implement experimentally are investigated.

2. Feedback using helical windings

Suppose that the feedback controlled conductors consist of a set of independent *helical windings*, such that at any given toroidal angle ϕ there are M windings located at poloidal angles

$$\theta_k=\frac{2\pi(k-1)}{M}+\frac{N}{M}\,\phi, \tag{139}$$

for $k=1$ to M. The set of windings clearly possesses M,N helical symmetry. As usual, it is convenient to adopt the single harmonic approximation, in which the shell stability indices for all harmonics, apart from the central harmonic m_0,n_0, take their vacuum values $-2|m|$. It is assumed that the windings are *resonant* with the central harmonic, so that $n_0M-m_0N=0$.

Suppose that each feedback winding is accompanied by a high resistance helical sensor loop, such that the kth loop is located at $\theta_k+\delta\theta$. Here, $d/r_w\ll\delta\theta\ll 2\pi/M$, where d is the diameter of the feedback windings. It is assumed that the feedback windings and the sensor loops possess the common minor radius r_w. The voltage (per unit length) generated by magnetic induction in the kth feedback winding is

$$V_k=\gamma\,\frac{\mu_0}{2\pi}\,\hat{I}e^{im_0\zeta_k}\left[\frac{M}{\Delta_w^{m_0,n_0}}-g(\sqrt{2\gamma\tau_w/M})\right.$$
$$\left.-\ln(2r_w/Md)-K_0(|m_0|/M)\right], \tag{140}$$

where use has been made of the results of Sec. IV C, including the assumed current distribution (86). Note that $\zeta_k=2\pi(k-1)/M$. Likewise, the voltage (per unit length) generated by magnetic induction in the kth sensor loop is

$$\tilde{V}_k=\gamma\,\frac{\mu_0}{2\pi}\,\hat{I}e^{im_0\zeta_k}\left[\frac{M}{\Delta_w^{m_0,n_0}}-\ln(1/M\,\delta\theta)-K_0(|m_0|/M)\right]. \tag{141}$$

Suppose that the signals generated in the sensor loops are integrated (from a time when the mode amplitude is negligibly small), amplified by a factor $1/\tau$, and then fed into the feedback windings. The signal fed into the kth winding is the *difference* between the signals derived from the $(k+1)$th and $(k-1)$th sensor loops. Thus, the modified circuit equation for the kth feedback winding is

$$V_k+\frac{\widetilde{V}_{k+1}-\widetilde{V}_{k-1}}{\gamma\tau}=RI_k, \tag{142}$$

where R is the resistance per unit length of the windings, and $I_k=\hat{I}e^{im_0\zeta_k}$ is the current flowing in the kth winding. Equations (140)–(142) yield the dispersion relation

$$\left[\gamma\left(\frac{1-\Delta_w^{m_0,n_0}/\Delta_c^{m_0,n_0}}{1-\Delta_w^{m_0,n_0}/\Delta_{c'}^{m_0,n_0}}\right)+i\Omega_w\right]\tau_w=\frac{\Delta_w^{m_0,n_0}}{1-\Delta_w^{m_0,n_0}/\Delta_{c'}^{m_0,n_0}}, \tag{143}$$

where

$$\tau_w=\frac{\mu_0 M}{2\pi R}, \tag{144}$$

and

$$\Omega_w=\frac{2\sin(2\pi m_0/M)}{\tau}. \tag{145}$$

Here,

$$\Delta_c^{m_0,n_0}=\frac{M}{g(\sqrt{2\gamma\tau_w/M})+\ln(2r_w/Md)+K_0(|m_0|/M)}, \tag{146}$$

and

$$\Delta_{c'}^{m_0,n_0}=\frac{M}{\ln(1/M\delta\theta)+K_0(|m_0|/M)}. \tag{147}$$

Note that the time constant τ_w, given by Eq. (144), is the same as the equivalent time constant (i.e., the time constant of a uniform shell of minor radius r_w which contains the same amount of metal as the feedback windings).

The dispersion relation (143) is (almost) the same (see Sec. V B) as that of a uniform resistive shell of effective time constant

$$\widetilde{\tau}_w=\tau_w\left(1+\frac{2|m_0|}{\Delta_{c'}^{m_0,n_0}}\right), \tag{148}$$

and effective radius

$$\widetilde{r}_w=r_w\left(1+\frac{2|m_0|}{\Delta_{c'}^{m_0,n_0}}\right)^{1/2|m_0|}, \tag{149}$$

which *rotates* poloidally with the effective angular rotation frequency Ω_w. In other words, the feedback scheme causes the set of helical windings to act like a fake rotating shell. Note that the effective rotation frequency, Ω_w, is directly proportional to the gain in the feedback circuits.

Suppose that the plasma is surrounded by a complete passive shell (e.g., the vacuum vessel) of radius r_v and time constant τ_v. This, in turn, is surrounded by the feedback controlled set of helical windings. Thus, $r_w>r_v>a$, where a is the minor radius of the edge of the plasma. The dispersion relation for the m_0,n_0 external kink mode is written[44] as

$$(\Delta_v-E_v)(\Delta_w-E_w)-(E_{vw})^2=0, \tag{150}$$

where

$$\Delta_v=\gamma\tau_v \tag{151}$$

is the dispersion relation of the passive shell, and [after rearranging Eq. (143)]

$$\Delta_w=\frac{(\gamma+i\Omega_w)\tau_w}{1+(\gamma\Delta_{c'}^{m_0,n_0}/\Delta_c^{m_0,n_0}+i\Omega_w)\tau_w/\Delta_{c'}^{m_0,n_0}} \tag{152}$$

is the dispersion relation of the feedback system. The remaining terms in Eq. (150) are given by

$$E_v=\frac{2|m_0|}{(r_c/r_v)^{2|m_0|}-1}-\frac{2|m_0|}{(r_w/r_v)^{2|m_0|}-1}, \tag{153a}$$

$$E_w=-\frac{2|m_0|(r_w/r_v)^{2|m_0|}}{(r_w/r_v)^{2|m_0|}-1}, \tag{153b}$$

$$E_{vw}=\frac{2|m_0|(r_w/r_v)^{|m_0|}}{(r_w/r_v)^{2|m_0|}-1}. \tag{153c}$$

Here, r_c is the critical radius defined in Sec. V B. The dispersion relation (150) is only valid in the limit where the coupling between the passive shell and the feedback windings is mediated predominantly by the central harmonic. In other words, when

$$\left(\frac{r_v}{r_w}\right)^{2|m_0+jM|}\ll 1 \tag{154}$$

for all $j\neq 0$, where j is an integer. This constraint is not particularly difficult to satisfy, unless the feedback windings are located very close to the passive shell.

It is both convenient and plausible to assume that the time constant of the passive shell is much longer than that of the fake shell. Thus, $\tau_v\gg\tau_w$. With this ordering, plus the ordering $\Omega_w\tau_w\sim O(1)$, the resistive shell mode root [i.e., the root with $\gamma\tau_v\sim O(1)$] of Eq. (150) can easily be shown to take the form

$$\gamma\tau_v\simeq\frac{2|m_0|}{(r_c/r_v)^{2|m_0|}-1}\times\left(\frac{1-\hat{\Omega}_w^2[(r_c/\widetilde{r}_w)^{2|m_0|}-1]/[1-(r_v/\widetilde{r}_w)^{2|m_0|}]}{1+\hat{\Omega}_w^2}\right)-i\,\frac{2|m_0|}{(\widetilde{r}_w/r_v)^{2|m_0|}-1}\,\frac{\hat{\Omega}_w}{1+\hat{\Omega}_w^2}, \tag{155}$$

where

$$\hat{\Omega}_w=\frac{\Omega_w\widetilde{\tau}_w}{2|m_0|}\,[1-(r_v/\widetilde{r}_w)^{2|m_0|}]. \tag{156}$$

It is clear from Eq. (155) that in the absence of feedback (i.e., $\Omega_w=0$) the resistive shell mode takes the form of a nonrotating mode growing on the time constant of the passive shell. Feedback causes the resistive shell mode to *propagate* in the direction of apparent rotation of the fake shell, but it also modifies the growth rate of the mode. If the effective radius of the fake shell w lies *beyond* the critical radius r_c, then feedback always causes an *increase* in the growth rate. However, if the effective radius lies *inside* the critical radius, then feedback causes the growth rate to *decrease*. In the latter case, there is a critical value of the effective angular rotation frequency of the fake shell, Ω_w, above which the resistive shell mode is stabilized. This critical rotation frequency is of order $1/\tau_w$. The corresponding critical ''voltage gain,'' $G=|\widetilde{V}_{k+1}-\widetilde{V}_{k-1}|/(|\gamma|\tau|\widetilde{V}_k|)$, in the feedback circuits (i.e., the ratio of the voltage fed into a particular feedback winding to that generated by magnetic induction in a neighboring sensor loop) is

$$G_c=\frac{\tau_v}{\tau_w}\left(\frac{r_w}{r_v}\right)^{2|m_0|}\frac{(r_c)^{2|m_0|}-(r_v)^{2|m_0|}}{(r_c)^{2|m_0|}-(\widetilde{r}_w)^{2|m_0|}}. \tag{157}$$

Thus, for $G>G_c$ the resistive shell mode is stabilized. The critical current which must be supplied by an individual feedback amplifier is

$$I_c\sim g_c\,\frac{2\pi r_w b_r}{\mu_0 M}, \tag{158}$$

where b_r is the perturbed radial magnetic field strength at radius r_w, and

$$g_c=2\,\frac{(r_w)^{2|m_0|}}{\sqrt{(r_c)^{2|m_0|}-(\widetilde{r}_w)^{2|m_0|}}\sqrt{(\widetilde{r}_w)^{2|m_0|}-(r_v)^{2|m_0|}}}. \tag{159}$$

Likewise, the critical power which must be supplied by an individual feedback amplifier is

$$P_c\sim g_c^2\,\frac{2\pi^2 r_w^2 R_0 b_r^2}{\mu_0\tau_w N}. \tag{160}$$

Note that these critical values are similar in magnitude to those obtained in the original feedback stabilization scheme where the feedback controlled conductors consist of a fine network of interconnected poloidal and toroidal wires. The number of amplifiers needed to implement the feedback scheme is equal to the number of *independent* helical windings, i.e., the required number of amplifiers is N.

Consider using the scheme outlined above to feedback stabilize an $n_0=1$ resistive shell mode. The feedback windings resonate with the mode provided that $M=Nm_0$, where N is the number of separate windings. When there is only *one* feedback winding (i.e., $N=1$), $m_0/M=1$, and it follows from Eqs. (147) and (149) plus Fig. 10 that $\Delta_{c'}^{m_0,n_0}=0$ and $\widetilde{r}_w\to\infty$. Thus, in this case, the effective radius of the fake shell tends to infinity, and the feedback scheme is, therefore, incapable of stabilizing the resistive shell mode. When there are *two* feedback windings (i.e., $N=2$), $m_0/M=1/2$, so $\widetilde{r}_w$ is finite, but it follows from Eq. (145) that $\Omega_w=0$. Thus, in this case, the fake shell does not rotate, and the feedback scheme remains incapable of stabilizing the resistive shell mode. When there are *three or more* feedback windings (i.e., $N>2$) it is easily demonstrated that $\widetilde{r}_w$ is finite and Ω_w is nonzero. Thus, in this case, the feedback scheme is capable of stabilizing the resistive shell mode. It is concluded that the *minimum* number of separate helical windings needed to implement the fake rotating shell feedback scheme is *three*. Note that in the case where there are two helical windings the feedback scheme only fails because the windings are equally spaced in helical angle [see Eq. (36)]. In fact, it is possible to implement the fake rotating shell feedback scheme using *two unequally spaced* helical windings. Regrettably, this configuration of windings lies beyond the scope of this paper, since it does not posses pure helical symmetry. On the other hand, it is impossible to implement the feedback scheme using a single helical winding.

Note, finally, that the feedback scheme outlined above fails completely for resistive shell modes which are *not resonant* with the helical coils. Such modes generate no signals in the helical sensor loops, so the fake shell does not rotate. More important, according to Sec. IV D, the effective radius of the fake shell is necessarily very large, in this case, because the currents induced in the helical windings are unable to flow in continuous unidirectional loops around the plasma. Thus, although it is possible to implement the fake rotating shell feedback scheme with as few as three equally spaced helical windings, driven by three power amplifiers, such a system is only capable of stabilizing those resistive shell modes which resonate with the windings.

3. Feedback using modular coils

Suppose that the feedback controlled conductors consist of a uniform array of *modular coils*, such that at any given toroidal angle there are M wire loops centered on poloidal angles

$$\zeta_k=\frac{2\pi(k-1)}{M}, \tag{161}$$

for $k=1$ to M. The kth loop contains two toroidally directed wires located at poloidal angles $\zeta_k\pm\Delta\theta/2$. The loops are assumed to be closely spaced in the toroidal direction, and such that their toroidal lengths are much less than the toroidal half-wavelength, $\pi R_0/n_0$, of the central harmonic. In this limit, there is no significant coupling of different toroidal harmonics by the loops. Thus, the set of feedback coils effectively possesses M, 0 helical symmetry. As usual, the single harmonic approximation is adopted in the following analysis.

Suppose that each feedback coil is accompanied by a high resistance sensor loop of equal area, such that the kth sensor loop is centered on $\zeta_k+\delta\theta$. Here, $d/r_w\ll\delta\theta\ll 2\pi/M$, where d is the diameter of the wires from which the feedback loops are constructed. It is assumed that the feedback and sensor loops are all located at minor radius r_w. The voltage (per unit toroidal length) generated by magnetic induction in the kth feedback loop (at $\phi=0$) is

$$V_k = 2\gamma\,\frac{\mu_0}{2\pi}\,\hat{I}e^{im_0\zeta_k}\Bigg[2M\,\sin^2(|m_0|\Delta\theta/2)\times\left(\frac{1}{\Delta_w^{m_0,n_0}}+\frac{1}{2|m_0|}\right)-g(\sqrt{4\gamma\tau_w/M})-\ln(2r_w\Delta\theta/d)-J_0(\Delta\theta,M,|m_0|)\Bigg], \tag{162}$$

where

$$J_0(\Delta\theta,M,|m_0|)=\sum_{j=1,\infty}\ln\left[1-\left(\frac{M\Delta\theta}{2\pi j}\right)^2\right]\times\cos(2\pi j|m_0/M). \tag{163}$$

Here, use has been made of the results of Sec. IV D. Likewise, the voltage (per unit toroidal length) generated by magnetic induction in the kth sensor loop (at $\phi=0$) is

$$\widetilde{V}_k = 2\gamma\,\frac{\mu_0}{2\pi}\,\hat{I}e^{im_0\zeta_k}\Bigg[2M\,\sin^2(|m_0|\Delta\theta/2)\left(\frac{1}{\Delta_w^{m_0,n_0}}+\frac{1}{2|m_0|}\right)-\ln(\Delta\theta/\delta\theta)-J_0(\Delta\theta,M,|m_0|)\Bigg]. \tag{164}$$

Suppose that the signals generated by the sensor loops are integrated (from a time when the mode amplitude is negligibly small), amplified by a factor $1/\tau$, and then fed into the feedback coils. The signal fed into the kth coil is the *difference* between the signals derived from the $(k+1)$th and $(k-1)$th sensor loops. Thus, the modified circuit equation for the kth feedback coil (at $\phi=0$) is

$$V_k+\frac{\widetilde{V}_{k+1}-\widetilde{V}_{k-1}}{\gamma\tau}=2RI_k, \tag{165}$$

where R is the resistance per unit length of the wires making up the feedback coils, and $I_k=\hat{I}e^{im_0\zeta_k}$ is the current flowing in the kth feedback coil (at $\phi=0$). Equations (162)–(165) yield the dispersion relation

$$\left[\gamma\left(\frac{1-\Delta_w^{m_0,n_0}/\Delta_c^{m_0,n_0}}{1-\Delta_w^{m_0,n_0}/\Delta_{c'}^{m_0,n_0}}\right)+i\Omega_w\right]\tau_w=\frac{\Delta_w^{m_0,n_0}}{1-\Delta_w^{m_0,n_0}/\Delta_{c'}^{m_0,n_0}}, \tag{166}$$

where

$$\tau_w=\sin^2(|m_0|\Delta\theta/2)\,\overline{\tau_w}, \tag{167}$$

and $\overline{\tau_w}=\mu_0 M/\pi R$, with

$$\Omega_w=\frac{2\sin(2\pi m_0/M)}{\tau}. \tag{168}$$

Here,

$$\Delta_c^{m_0,n_0}=\frac{2M\,\sin^2(|m_0|\Delta\theta/2)}{g(\sqrt{2\gamma\overline{\tau_w}/M})+\ln(2r_w\Delta\theta/d)+J_0(\Delta\theta,M,|m_0|)-\sin^2(|m_0|\Delta\theta/2)M/|m_0|}, \tag{169}$$

and

$$\Delta_{c'}^{m_0,n_0}=\frac{2M\,\sin^2(|m_0|\Delta\theta/2)}{\ln(\Delta\theta/\delta\theta)+J_0(\Delta\theta,M,|m_0|)-\sin^2(|m_0|\Delta\theta/2)M/|m_0|}. \tag{170}$$

Note that the time constant $\overline{\tau_w}$ is the same as the equivalent time constant (i.e., the time-constant of a uniform shell of minor radius r_w which contains the same amount of metal as the feedback coils).

The dispersion relation (166) is (almost) the same as that of a uniform resistive shell of effective time constant $\widetilde{\tau}_w$ [given by Eq. (148)], and effective radius $\widetilde{r}_w$ [given by Eq. (149)], which rotates poloidally with the effective angular rotation frequency Ω_w. Thus, the feedback scheme causes the set of feedback coils to act like a ''fake rotating shell.'' Note that the effective rotation frequency, Ω_w, is again directly proportional to the gain in the feedback circuits.

Suppose that the plasma is surrounded by a complete passive shell of radius r_v and time constant τ_v. This, in turn, is surrounded by the array of feedback coils. In the limit in which the coupling between the passive shell and the feedback coils is mediated predominantly by the central harmonic [see Eq. (154)], the dispersion relation for the m_0,n_0 external kink mode takes the form given by Eq. (150). In the physically relevant limit $\tau_v\gg\tau_w$, the growth rate of the resistive shell mode is determined by Eq. (155). It is easily seen that, as long as the effective radius of the fake rotating shell, $\widetilde{r}_w$, lies inside the critical radius, r_c, the feedback scheme is capable of stabilizing the resistive shell mode. In fact, stabilization is achieved once the effective rotation frequency of the fake shell, Ω_w, exceeds a critical value which is of order $1/\tau_w$. The corresponding critical voltage gain, $G=|\widetilde{V}_{k+1}-\widetilde{V}_{k-1}|(|\gamma|\tau\widetilde{V}_k)$, in the feedback circuits (i.e., the ratio of the voltage fed into a particular feedback coil to that generated by magnetic induction in a neighbouring sensor loop) is given by Eq. (157). The critical current which must be supplied by an individual feedback amplifier is

$$I_c\sim g_c\,\frac{\pi r_w b_r}{\mu_0 M\,\sin(|m_0|\Delta\theta/2)}, \tag{171}$$

where b_r is the perturbed radial magnetic field strength at radius r_w, and the factor g_c is specified by Eq. (159). Likewise, the critical value of the *total* power supplied by the feedback amplifiers is

$$P_c\sim g_c^2\,\frac{2\pi^2 r_w^2 R_0 b_r^2}{\mu_0\overline{\tau_w}\,\sin^2(|m_0|\Delta\theta/2)}. \tag{172}$$

The minimum allowable number of feedback coils in the toroidal direction is $2n_0+1$.[43] Thus, the number of amplifiers needed to implement the feedback scheme, which is equal to the number of feedback coils, is at least $(2n_0+1)M$.

Consider using the scheme outlined above to feedback stabilize an m_0,n_0 resistive shell mode. It is clear from Eq. (168) that if $2m_0=jM$, where j is an integer, then $\Omega_w=0$. Thus, in this case, the fake shell does not rotate, and the feedback scheme is incapable of stabilizing the resistive shell mode. It follows that the *minimum* number of feedback coils in the poloidal direction needed to construct a fake rotating shell is *three* (i.e., $M\geqslant 3$). It is clear from Eqs. (149) and (170) that the effective radius, $\tilde{r}_w$, of the fake shell tends to infinity when $|m_0|\Delta\theta/2=k\pi$, where k is an integer. Thus, in this case, the feedback scheme is also incapable of stabilizing the resistive shell mode. On the other hand, $\tilde{r}_w$ is minimized (as a function of $\Delta\theta$) whenever $|m_0|\Delta\theta/2=(k+1/2)\pi$, where k is an integer. In this situation, the critical current and critical total power which the feedback amplifiers must put out in order to stabilize the resistive shell mode are similar in magnitude to the values obtained when the feedback controlled conductors consist of a fine network of wires, or a set of resonant helical windings. The critical current and critical total power increase significantly above these values when $|m_0|\Delta\theta/2\neq(k+1/2)\pi$ [see Eqs. (171) and (172)]. It follows that a modular coil feedback scheme works optimally when the poloidal extent of each feedback coil is an odd integer multiple of the poloidal half-wavelength of the central harmonic. The feedback scheme fails completely when the poloidal extent of each feedback coil is an even integer multiple of the poloidal half-wavelength of the central harmonic. Note, in particular, that the feedback scheme only works poorly when the poloidal extent of each coil is much smaller than the poloidal half-wavelength of the central harmonic.

For the case of a 3, 1 resistive shell mode, the minimum number of feedback coils in the poloidal direction needed to construct a fake rotating shell is *four*. The optimum poloidal angular extent of each coil is 60°. Note that this configuration of coils is incapable of stabilizing the 2, 1 or the 4, 1 resistive shell modes, since the fake shell appears stationary to these modes. However, with *five* feedback coils in the poloidal direction, each of poloidal angular extent 60°, it is possible to construct a fake rotating shell which is capable of *simultaneously* stabilizing the 2, 1, 3, 1, and 4, 1 resistive shell modes. This scheme works optimally for the 3, 1 mode, since the poloidal angular extent of each feedback coil matches the poloidal half-wavelength of this mode. The scheme works less efficiently for the 2, 1 and 4, 1 modes, i.e., the critical currents and critical total power which the feedback amplifiers must put out in order to stabilize these modes are larger than they would have been were the feedback scheme optimized for these modes. The minimum number of feedback coils in the toroidal direction needed to implement this scheme is *three*. Thus, the total number of feedback coils and power amplifiers required by this particular feedback stabilization scheme is at least *fifteen*.

4. Summary and discussion

The original fake rotating shell feedback stabilization scheme, in which the feedback controlled conductors consist of a *fine* network of interconnected toroidal and poloidal wires surrounding the plasma, is capable of stabilizing a resistive shell mode of *arbitrary* helicity at relatively low values of the current and total power supplied by the feedback amplifiers. The main disadvantage of this scheme is the very large number of feedback amplifiers (i.e., one per network cell) which are needed to implement it. Another problem arises from the fact that the feedback controlled conductors link the primary induction winding of the tokamak: the primary winding is likely to drive large eddy currents in the network as the plasma current is ramped up or down.

Section V C 2 discusses a modified fake rotating shell feedback stabilization scheme in which the feedback controlled conductors consist of a set of independent helical windings. The main advantage of this modified scheme is the very small number (i.e., as few as three) of feedback amplifiers needed to implement it. The current and total power requirements are similar to those of the original scheme. The main disadvantage of the modified scheme is that it is only effective for the relatively small class of resistive shell modes which *resonate* with the helical windings. In fact, the scheme fails completely for nonresonant modes. Furthermore, the feedback controlled conductors still link the primary winding.

Section V C 3 discusses a modified fake rotating shell stabilization scheme in which the feedback controlled conductors consist of an array of modular coils. The number of feedback amplifiers needed to implement this scheme is relatively small, but not as small as the number of amplifiers needed to implement the helical winding based scheme. On the other hand, a modular coil based feedback stabilization scheme is effective for resistive shell modes possessing a wide range of different helicities. The current and total power requirements are similar to those of the original scheme for the relatively small class of resistive shell modes where the poloidal extent of each feedback coil is an odd integer multiple of the poloidal half-wavelength of the mode. The feedback scheme fails completely for a second relatively small class of modes where the poloidal extent of each feedback coil is an even integer multiple of the poloidal half-wavelength of the mode. For the remaining modes, the feedback scheme is effective, but the current and total power requirements on the feedback amplifiers *significantly exceed* those of the original feedback scheme. Modular coils do not link the primary induction winding of the tokamak, so there is no danger of eddy currents being driven in the feedback coils as the plasma current is ramped up or down.

All three of the fake rotating shell feedback stabilization schemes described above have their own peculiar set of advantages and disadvantages. On balance, the scheme which uses *modular* feedback coils is the one most likely to succeed experimentally.

D. Discussion

It is clear from Secs. V B and V C that the theory presented in Secs. II–IV is *highly relevant* to both the design of

incomplete passive stabilizing shells and the design of active feedback systems (for external modes) which employ relatively small numbers of feedback coils.

VI. SUMMARY AND DISCUSSION

Section II introduces the basic concepts needed to determine the influence of a partial resistive shell on the growth rate of the external kink mode in a low-β, large aspect-ratio, circular flux-surface tokamak. A rather heuristic derivation is given (in Sec. II E) of the fundamental dispersion relation (27) for the resistive shell mode. It turns out that this dispersion relation holds for all partial resistive shells, provided that only a single resistive shell mode (the m_0,n_0 mode, say) is intrinsically unstable. This condition is easily satisfied in tokamaks. The dispersion relation (27) allows a partial resistive shell to be replaced by a complete *effective shell* of radius $\widetilde{r}_w$ and time constant $\widetilde{\tau}_w$. The relationship between the radius and time constant of the effective shell and those of the actual shell depends on the distribution of gaps in the actual shell. In some cases, this relationship is found to take a particularly simple form [see Eqs. (28) and (33)] in which $\widetilde{r}_w$ and $\widetilde{\tau}_w$ only depend on the area fraction of gaps in the shell, and are independent of the actual arrangement of gaps. Note that the radius of the effective shell always exceeds the radius of the actual shell. The effective radius $\widetilde{r}_w$ can be used to parametrize the ability of a partial shell to moderate the growth of the external kink mode. If $\widetilde{r}_w > r_c$, then the external kink mode is unstable with an ideal growth rate, whereas if $\widetilde{r}_w < r_c$ the ideal mode is stable but the resistive shell mode is unstable, growing on the relatively long time constant of the shell. Here, r_c is the critical radius of the m_0,n_0 mode; i.e., r_c is the largest radius at which a complete perfectly conducting shell is able to stabilize the m_0,n_0 ideal external kink mode. It is clear that the smaller the effective radius of a partial shell, the better able the shell is to moderate the growth of the external kink mode.

Section III describes in detail, how the analysis of Sec. II can be employed to calculate the growth rate of the resistive shell mode for the case of a partial shell containing *helical* gaps. In fact, the problem reduces to a straightforward two-dimensional matrix eigenvalue problem. It is necessary to make a distinction between resonant and nonresonant shells. In the former case, it is possible for m_0,n_0 eddy currents to flow in unidirectional continuous loops around each helical segment of the shell, whereas in the latter case this is impossible because the helicity of the shell does not match that of the m_0,n_0 mode. For nonresonant partial shells, the radius of the effective shell is found to depend only on the area fraction of gaps, provided that the dimensions all metal and gaps sections of the shell are larger than the poloidal half-wavelength of the m_0,n_0 mode. Nonresonant shells for which this condition is not satisfied are found to possess larger effective radii than similar nonresonant shells (i.e., nonresonant shells containing the same area fraction of gaps) for which this condition is satisfied. In other words, the former type of shell is less able to moderate the growth of the external kink mode than the latter type. Resonant shells are found to perform better than similar nonresonant shells (i.e., the effective radii of the former type of shells are smaller than those of the latter type), provided that they contain *two* or *more* independent helical paths per helical period of the m_0,n_0 mode. Resonant shells which contain only *one* helical path per helical period actually perform worse than similar nonresonant shells. As the number of helical paths per helical period increases, the radius of the effective shell asymptotes to that of the actual shell. This effect takes place irrespective of the dimensions of the metal and gaps sections compared to the poloidal half-wavelength of the m_0,n_0 mode. Thus, a resonant partial shell possessing very many helical paths per helical period of the m_0,n_0 mode is just as effective at moderating the growth of the external kink mode as a complete shell with the same minor radius: this remains the case even in the limit in which the area fraction of gaps in the partial shell tends to unity.

Section IV is devoted to the study of skeletal shells constructed from thin helical wires or helical wire loops. Analytic expressions are obtained for the effective radius and effective time constant of the shell in both cases. This analysis is worthwhile for two main reasons. First, it allows a qualitative understanding of the behavior of partial shells containing helical gaps, in the limit in which the fraction of gaps tends to unity. Second, and more important, such analysis is a necessary prerequisite for evaluating the effectiveness of realistic feedback control schemes for external modes.

Section V describes various applications of the theory presented in Secs. II–IV. In Sec. V B the theory is used to derive some general rules regarding the design of passive stabilizing shells. For nonresonant shells the optimum performance is achieved when the dimensions of all metal and gap sections exceed the poloidal half-wavelength of the m_0,n_0 mode. In this case, the radius of the effective shell depends only on the area fraction of gaps contained in the shell, and is always greater than the radius of the actual shell. For resonant shells the optimum performance is achieved when there are very many (i.e., at least two) independent helical paths through the shell per helical period of the m_0,n_0 mode. In this case, the radius of the effective shell approaches that of the actual shell. Thus, it is always possible to improve the performance of a nonresonant shell by installing ''jump leads'' between the separate metal sections, so as to form at least two helical paths per helical period of the m_0,n_0 mode.

In Sec. V C the theory is used to evaluate two feedback stabilization schemes for the resistive shell mode, both of which employ a relatively small set of independent feedback coils. These schemes are both variants on the fake rotating shell stabilization scheme described in Ref. 43. The original scheme is capable of stabilizing any resistive shell mode, but requires a very large number of feedback amplifiers. Section V C 2 describes a scheme in which the feedback controlled conductors consist of a set of independent helical windings. This scheme can be effective with a few as *three* feedback windings (and power amplifiers), but is only capable of stabilizing the relatively small set of resistive shell modes which resonate with the windings. Section V C 3 describes a scheme in which the feedback controlled conductors consist of an array of modular coils. In order to be effective, this scheme requires slightly more feedback coils (and power am-

plifiers) than the helical winding based scheme. On the other hand, the modular coil based scheme is capable of stabilizing a far wider range of resistive shell modes.

In conclusion, the theory presented in this paper is of great importance to both the design of passive stabilizing shells and the design of active feedback systems (for external modes) in tokamaks.

All of the analysis presented in this paper depends crucially on the validity of the ''thin shell'' approximation (see Sec. II E). This approximation holds provided that

$$\frac{\delta_w}{r_w} \ll \Delta_w^{m,n} \ll \frac{r_w}{\delta_w}, \tag{173}$$

where r_w and δ_w are the minor radius and thickness of the conducting sections of the shell, respectively. Here, $\Delta_w^{m,n}$ is the shell stability index for the m,n harmonic (see Sec. II). The above inequality must be satisfied for all harmonics coupled by the eddy currents excited in the shell. For the case of the resistive shell mode, the inequality only breaks down in a relatively narrow range of parameter space just before the marginal stability point for the ideal external kink mode is reached. Here, it is assumed, as seems reasonable, that the thickness of the shell is much less than its minor radius (i.e., $\delta_w/r_w \ll 1$). Thus, the situation which is of primary practical importance (i.e., that where the system lies well away from the marginal stability point for the ideal mode in parameter space, so that the resistive shell mode grows on some characteristic L/R time of the shell) is governed by the thin shell approximation. Note that the thin shell approximation can easily be invalidated for the case of a rapidly rotating tearing mode interacting with a resistive shell. Thus, the analysis presented in this paper probably needs to be extended in order to deal effectively with this case: this subject will be discussed in a future publication.

The analysis presented in this paper is only valid for low-β, large aspect-ratio, circular flux-surface tokamaks. In high-β, finite aspect-ratio tokamaks it is generally found that resistive shell modes are far more sensitive to gaps in the shell situated on the outboard midplane compared to gaps situated on the inboard mid-plane.[45] This effect, which is essentially due to the large outward Shafranov shift of the innermost flux surfaces in high-β tokamak plasmas, does not occur in this paper, where the flux surfaces are modeled as concentric circles. However, the effect can be very conveniently simulated by simply shifting the plasma equilibrium with respect to the shell, so that the spacing between the plasma and the shell is smaller on the outboard midplane than on the inboard midplane: this subject will also be discussed in a future publication.

ACKNOWLEDGMENTS

Most of the work described in this paper was performed while the author was visiting General Atomics (La Jolla, CA) during the summer of 1996. The author gratefully acknowledges Dr. Vincent Chan (General Atomics) for making this visit possible. The author also acknowledges Dr. Torkil H. Jensen (General Atomics) and Dr. Neil Pomphrey (Princeton Plasma Physics Laboratory, NJ) for helpful discussions during the preparation of this paper. This research was funded by the U.S. Department of Energy under Contract No. DE-FG05-96ER-54346.

[1] J. P. Goedbloed, D. Pfirsch, and H. Tasso, Nucl. Fusion **12**, 649 (1972).
[2] M. Tanaka, T. Tuda, and T. Takeda, Nucl. Fusion **13**, 119 (1973).
[3] T. Sometani and K. Fukagawa, Jpn. J. Appl. Phys. **17**, 2035 (1978).
[4] G. F. Nalesso and S. Costa, Nucl. Fusion **20**, 443 (1980).
[5] A. H. Boozer, Phys. Fluids **24**, 1387 (1981).
[6] J. P. Freidberg, J. P. Goedbloed, and R. Rohatgi, Phys. Rev. Lett. **51**, 2105 (1983).
[7] T. H. Jensen and M. S. Chu, J. Plasma Phys. **30**, 57 (1983).
[8] F. Gnesotto, G. Miano, and G. Rubinacci, IEEE Trans. Magn. **MAG-21**, 2400 (1985).
[9] G. Miller, Phys. Fluids **28**, 560 (1985).
[10] C. G. Gimblett, Nucl. Fusion **26**, 617 (1986).
[11] P. H. Rutherford, *Basic Physical Processes of Toroidal Fusion Plasmas*, Proceedings of Course and Workshop, Varenna, 1985 (Commission of the European Communities, Brussels, 1986), Vol. 2, p. 531.
[12] L. E. Zakharov and S. V. Putvinskii, Sov. J. Plasma Phys. **13**, 68 (1987).
[13] Y. L. Ho and S. C. Prager, Phys. Fluids **31**, 1673 (1988).
[14] G. Berge, L. K. Sandal, and J. A. Wesson, Phys. Scr. **40**, 173 (1989).
[15] S. W. Haney and J. P. Freidberg, Phys. Fluids B **1**, 1637 (1989).
[16] K. Hattori, J. Phys. Soc. Jpn. **58**, 2227 (1989).
[17] T. C. Hender, C. G. Gimblett, and D. C. Robinson, Nucl. Fusion **29**, 1279 (1989).
[18] M. Persson and A. Bondeson, Nucl. Fusion **29**, 989 (1989).
[19] C. G. Gimblett, Plasma Phys. Control. Nucl. Fusion **31**, 2183 (1989).
[20] D. Edery and A. Samain, Plasma Phys. Control. Nucl. Fusion **32**, 93 (1990).
[21] M. F. F. Nave and J. A. Wesson, Nucl. Fusion **30**, 2575 (1990).
[22] H. Zohm, A. Kallenbach, H. Bruhns, G. Fussmann, and O. Klüber, Europhys. Lett. **11**, 745 (1990).
[23] A. F. Almagri, S. Assadi, S. C. Prager, J. S. Sarff, and D. W. Kerst, Phys. Fluids B **4**, 4081 (1992).
[24] R. Fitzpatrick, Nucl. Fusion **33**, 1049 (1993).
[25] A. Bondeson and D. J. Ward, Phys. Rev. Lett. **72**, 2709 (1994).
[26] R. Betti and J. P. Freidberg, Phys. Rev. Lett. **74**, 2949 (1995).
[27] R. Fitzpatrick and A. Y. Aydemir, Nucl. Fusion **36**, 11 (1996).
[28] C. Kessel, J. Manickam, G. Rewoldt, and W. M. Tang, Phys. Rev. Lett. **72**, 1212 (1994).
[29] The conventional definition of this parameter is $\beta = 2\mu_0 \langle p \rangle / \langle B^2 \rangle$, where $\langle \cdots \rangle$ denotes a volume average, p is the plasma pressure, and B is the magnetic field strength.
[30] R. J. Bickerton, J. W. Connor, and J. B. Taylor, Nat. Phys. Sci. **229**, 110 (1979).
[31] R. J. Goldston, Phys. Plasmas **3**, 1794 (1996).
[32] H. P. Furth, J. Killeen, and M. N. Rosenbluth, Phys. Fluids **6**, 459 (1963).
[33] P. H. Rutherford, Phys. Fluids **16**, 1903 (1973).
[34] The standard large aspect-ratio, low-β tokamak ordering is $R_0/a \gg 1$ and $\beta \sim (a/R_0)^2$, where R_0 and a are the major and minor radii of the plasma, respectively.
[35] M. Okabayashi, N. Pomphrey, J. Manickam, D. J. Ward, R. E. Bell, R. E. Hatcher, R. Kaita, S. M. Kaye, H. W. Kugel, B. LeBlanc, F. M. Levinton, D. W. Roberts, S. Sesnic, Y. Sun, and H. Takahashi, Nucl. Fusion **36**, 1167 (1996).
[36] M. K. Vijaya Sankar, E. Eisner, A. Garofalo, D. Gates, T. H. Ivers, R. Kombargi, M. E. Mauel, D. Maurer, D. Nadle, G. A. Navratil, and Q. Xiao, J. Fusion Energy **12**, 303 (1993).
[37] R. C. Davidson, R. J. Goldston, G. H. Neilson, and K. I. Tomassen, Phys. Plasmas **2**, 2417 (1995).
[38] P.-H. Rebut, Fusion Technol. **27**, 3 (1995).
[39] J. A. Wesson, Nucl. Fusion **18**, 87 (1978).
[40] R. Fitzpatrick, Phys. Plasmas **1**, 2931 (1994).
[41] W. A. Newcomb, Ann. Phys. (N.Y.) **10**, 232 (1960).
[42] R. Fitzpatrick, *Plasma Physics and Controlled Nuclear Fusion Research, 1988*, Proceedings of the 15th International Conference, Seville, 1994 (International Atomic Energy Agency, Vienna, 1996), Vol. 3, p. 245.
[43] R. Fitzpatrick and T. H. Jensen, Phys. Plasmas **3**, 2641 (1996).
[44] R. Fitzpatrick, Phys. Plasmas **4**, 2519 (1997).
[45] D. J. Ward, Phys. Plasmas **3**, 3653 (1996).